NETWORK LISER

Discussion Paper Series

IZA DP No. 18595

April 2026

Harnessing Genetic Variants for Local Average Treatment Effect Estimation

Michela Bia
Luxembourg Institute of Socio-Economic Research (LISER), University of Luxembourg and IZA@LISER

Giorgia Menta
Luxembourg Institute of Socio-Economic Research (LISER) and IZA@LISER

Martin Huber
University of Fribourg

Conchita D'Ambrosio
University of Luxembourg

IZA DP No. 18595 April 2026

Harnessing Genetic Variants for Local Average Treatment Effect Estimation*

Abstract

When multiple instruments are available, conventional instrumental variable estimators aggregate across potentially heterogeneous margins of compliance and may yield effects that lack a clear economic interpretation. The problem is compounded when some instruments violate the exclusion restriction, as is common in certain empirical contexts such as those using genetic variants as instrumental variables. We propose a clustering-based plurality framework for instrumental variable estimation that jointly addresses instrument heterogeneity and invalid instruments. Rather than imposing a single common causal parameter, our approach groups instruments according to similarity in first-stage and applies a plurality rule on subgroups with similar reduced-form to identify locally valid subsets. This yields a collection of margin-specific local average treatment effects instead of a single pooled estimate. We extend plurality-based identification to settings with non-mutually exclusive instruments, such as Mendelian Randomization designs where all individuals are exposed to all genetic variants. We illustrate the method in a two-sample Mendelian Randomization analysis of the causal effect of educational attainment on smoking participation. Our results confirm a negative causal effect of education on smoking that remains robust under pleiotropy-robust estimators, while revealing substantial heterogeneity across instrument defined margins that is masked by pooled IV approaches. The framework provides a unified way to interpret and validate high-dimensional instruments in the presence of both treatment effect heterogeneity and potential violations of exclusion.

JEL classification

C31, C36, I10

Keywords

causal inference, LATE, heterogeneous treatments, instrumental variables, Mendelian Randomization

Corresponding author

Michela Bia
michela.bia@liser.lu; michela.bia@ext.uni.lu

* Michela Bia acknowledges financial support from the Inter Mobility IN Program: "Causal Mediation Analysis and Machine Learning based estimators (CAME)", funded by the Luxembourg National Research Fund.

1 Introduction

Instrumental variable (IV) methods are central to empirical economics when treatment assignment is endogenous. When many instruments are available, however, IV estimation ceases to identify a single causal effect. Each instrument shifts treatment along a potentially distinct margin of compliance, and standard multi-instrument estimators mechanically aggregate across these margins. In the presence of treatment effect heterogeneity, this aggregation delivers a weighted average of instrument-specific local effects whose economic interpretation is often unclear. When some instruments are invalid, the problem is compounded: pooling across heterogeneous and misspecified instruments may obscure meaningful local structure or even reverse the sign of the underlying effects. The econometric challenge is therefore not only how to estimate a causal parameter, but which instruments identify which margins, and which of them should be trusted.

In this paper, we propose a clustering-based plurality framework that addresses these challenges jointly. Rather than imposing a single common causal parameter across all instruments, we allow instruments to index different margins of variation. We first group instruments according to similarity in how strongly and in which direction they shift treatment. Within each group, we then apply a plurality rule: the largest internally coherent subset is treated as locally valid, while smaller inconsistent subsets are discarded. This yields a collection of margin-specific causal effects instead of a single pooled estimate. By enforcing validity locally rather than globally, our procedure accommodates both treatment effect heterogeneity and potentially invalid instruments. The starting point of our approach is a simple observation from the LATE framework (Imbens and Angrist, 1994). When treatment effects vary, each instrument identifies the effect for the individuals whose treatment status it shifts. With multiple instruments, there is no reason to expect these local effects to coincide. Yet conventional two-stage least squares aggregates across instruments mechanically, producing a weighted average that may correspond to no economically meaningful group (Alvarez and Toneto, 2024; Mogstad and Torgovitsky, 2024; Imbens and Angrist, 1994). Our framework treats this heterogeneity as informative rather than problematic: instruments that behave similarly in both first-stage and reduced-form relationships are interpreted as identifying a common margin of compliance.

We build on Apfel et al. (2023), who develop a plurality-based clustering approach in settings with mutually exclusive instruments, such as judges randomly assigned to cases. In that environment, each individual is exposed to exactly one instrument, and heterogeneity arises across disjoint complier populations defined by instrument assignment. We extend this logic to settings with non-mutually exclusive instruments. In many modern applications — especially genetic designs — every individual is exposed to all instruments simultaneously. Heterogeneity therefore does not arise from partitioning the population into separate complier groups. Instead, it reflects differences in how instruments shift the underlying propensity for treatment. Our contribution is to adapt plurality-based identification to this overlapping-instrument environment.[1]

These issues are particularly salient in Mendelian Randomization (MR), a rapidly growing literature that uses genetic variants as instruments (Davey Smith and Hemani, 2014). A genetic variant typically refers to a Single Nucleotide Polymorphism (SNP), a position in the DNA sequence at which individuals may carry different alleles. Because individuals inherit one allele from each parent, the instrument is measured as the number of copies — zero, one, or two — of a given "effect allele." Large genome-wide association studies (GWAS) estimate how strongly each SNP is associated with traits such as educational attainment. These estimated associations serve as first-stage relationships in MR analyses.

The appeal of MR is that genetic variants are approximately randomly assigned at conception, conditional on ancestry controls. This makes them attractive candidates for IV. However, genetic instruments face a distinctive challenge: horizontal pleiotropy. For instance, a variant that predicts education may also influence smoking through inde-

[1] While our algorithm partitions SNPs into mutually exclusive clusters for estimation, individuals remain simultaneously exposed to all variants; mutual exclusivity arises only at the instrument-classification level, not at the level of treatment exposure.

pendent biological or behavioral pathways. When many SNPs are used as instruments, some degree of pleiotropy is almost inevitable. The assumption that all variants satisfy the exclusion restriction is therefore rarely credible. Because horizontal pleiotropy is pervasive, a large literature has developed methods for estimation with some invalid instruments. Early econometric contributions formalized identification under majority or plurality validity conditions (Kang et al., 2016; Windmeijer et al., 2019). In the MR context, the weighted median estimator assumes that more than half of the instrument weight comes from valid variants (Bowden et al., 2016), while the mode-based estimator relies on a plurality assumption: the largest group of variants sharing the same implied causal estimate is assumed to be valid (Hartwig, Davey Smith and Bowden, 2017). Related contamination-mixture approaches similarly identify a dominant cluster of ratio estimates (Burgess et al., 2020). A common feature of these methods is that they target a single structural parameter, treating invalid variants as outliers around a common causal effect.

Our framework differs in a fundamental way. Rather than assuming that all valid instruments share the same underlying parameter, we first group instruments according to how they shift treatment (the first stage) and then apply a plurality rule within each group. When instruments shift treatment at different margins, the underlying causal effect may vary in magnitude — and, in principle, even in sign — across subpopulations. In that case, forcing all valid instruments to agree on a single estimate may obscure meaningful heterogeneity. By clustering instruments first on how they shift treatment and then on how they relate to the outcome, we allow different clusters to identify different local effects, while applying a plurality rule within each cluster to enforce validity. In this sense, we extend plurality-based identification from a single-parameter setting to a heterogeneous LATE environment. Validity is therefore enforced locally rather than globally, and different clusters may identify distinct local effects.

We illustrate our framework by estimating the causal effect of education on smoking using a two-sample Mendelian Randomization design. In a two-sample MR design, the first-stage association between each genetic variant and education is estimated in one

GWAS, while the reduced-form association between the same variants and smoking is estimated in a separate GWAS. The causal effect is then obtained by combining these variant-specific first-stage and reduced-form coefficients in a Wald-type IV estimator. In practice, this means that estimation is conducted using the reported regression coefficients for each variant, rather than individual-level data.

The relationship between educational attainment and smoking behavior has been extensively studied in both economics and epidemiology. Reform-based IV studies find that increases in compulsory schooling reduce smoking participation (Clark and Royer, 2013; Davies et al., 2018), suggesting that education may function as a public health intervention. In the MR literature, a prominent two-sample analysis using early GWAS of educational attainment (Okbay et al., 2016) and smoking phenotypes from the Tobacco and Genetics Consortium (Tobacco and Genetics Consortium, 2010) reports a negative causal effect of education on smoking initiation and heaviness (Gage et al., 2018). However, some of the estimates in that study depend on different Mendelian Randomization (MR) methods, like MR-Egger. This highlights concerns about pleiotropy and the reliability of the instruments used. More recent work suggests that the education–smoking relationship is unlikely to be fully mediated by cognitive ability (Sanderson et al., 2019).

Using larger and more recent GWAS, we revisit this relationship in a higher-powered setting. For educational attainment, we use the latest GWAS based on nearly three million individuals (Okbay et al., 2022). For smoking behavior, we use summary statistics from Karlsson Linnér et al. (2019), which include an "ever smoker" phenotype based on over one million individuals from UK Biobank and related cohorts. The substantially larger sample sizes relative to early MR studies increase statistical power and allow us to examine heterogeneity across instrument-defined margins of educational variation. Our estimates confirm a negative causal effect of education on smoking participation and remain stable under pleiotropy-robust estimators.

This paper contributes to the literature in several ways. First, we contribute to the econometrics of instrumental variables with heterogeneous treatment effects. The LATE framework (Imbens and Angrist, 1994; Angrist, Imbens and Rubin, 1996) establishes that different instruments identify different local causal effects. Subsequent work has clarified how multi-instrument 2SLS aggregates across margins in ways that complicate interpretation (Heckman and Vytlacil, 2005; Mogstad, Torgovitsky and Walters, 2021). We provide a data-driven procedure that maps instruments to distinct margins of variation and estimates multiple local causal effects rather than collapsing them into a single pooled estimate.

Second, we contribute to the literature on instrumental variables with some invalid instruments. A growing body of work establishes identification under majority or plurality validity conditions (Kang et al., 2016; Windmeijer et al., 2019). In the MR context, weighted median and mode-based estimators similarly rely on majority or plurality assumptions (Bowden et al., 2016; Hartwig, Davey Smith and Bowden, 2017), while contamination-mixture approaches identify a dominant cluster of ratio estimates (Burgess et al., 2020). These methods are designed to recover a single structural parameter in the presence of pleiotropy. In contrast, we extend plurality logic to an environment with heterogeneous margin-specific effects and non-mutually exclusive instruments, enforcing validity locally within instrument-defined clusters.

Third, we extend the plurality-based clustering approach of Apfel et al. (2023) to high-dimensional instrument environments where instruments overlap across individuals. While their framework is developed for mutually exclusive instruments such as judges, we adapt it to settings — particularly genetic designs — in which all individuals are simultaneously exposed to all instruments. Fourth, we contribute to the Mendelian Randomization literature by providing a complementary approach to robust estimation under horizontal pleiotropy. Rather than selecting a single dominant causal estimate, our framework recovers multiple margin-specific effects, allowing for treatment effect heterogeneity across instrument-induced margins of educational variation.

The remainder of the paper is organized as follows. Section 2 introduces the model and assumptions employed in the identification of LATEs. Section 3 describes the methods, while Section 4 introduces the data, the empirical application and our findings. We provide concluding remarks in Section 5.

2 Econometric Strategy

2.1 Notation

A genetic variant typically refers to a Single Nucleotide Polymorphism (SNP), a location in the DNA sequence at which individuals may carry different alleles. Because individuals inherit one allele from each parent, SNPs are coded as the number of copies (0, 1, or 2) of a given effect allele.

In our analysis, we study the causal effect of education D on smoking behavior Y using genetic variants $\mathbf{Z}$ as instrumental variables. Estimated associations between each genetic variant and the traits of interest come from genome-wide association study (GWAS) summary statistics. GWAS estimate, for each SNP, the association between allelic dosage and a phenotype using large samples of genotyped individuals. The resulting regression coefficients can be interpreted as per-allele effects on a standardized phenotype.

In the instrumental variable framework, the association between each SNP and educational attainment constitutes the first stage, while the association between the same SNP and smoking behavior constitutes the reduced form. These SNP-level regression coefficients provide the ingredients for Wald-type IV estimators constructed without access to individual-level data.

More formally, let $j = 1, \ldots, J$ index SNPs. For each SNP j, let β_{Dj} denote the population association between SNP j and education (the first-stage parameter), and let β_{Yj} denote the population association between SNP j and smoking (the reduced-form parameter). In practice, these population parameters are not observed. Instead, we observe their GWAS estimates and associated standard errors,

$$\hat{\beta}_{Dj},\ \hat{\sigma}_{Dj} \qquad \text{and} \qquad \hat{\beta}_{Yj},\ \hat{\sigma}_{Yj},$$

where $\hat{\beta}_{Dj}$ and $\hat{\beta}_{Yj}$ denote the estimated first-stage and reduced-form coefficients reported in the education and smoking GWAS, respectively, and $\hat{\sigma}_{Dj}$ and $\hat{\sigma}_{Yj}$ their corresponding standard errors.

A convenient reduced-form representation at the population level is

$$\beta_{Yj} = \theta\,\beta_{Dj} + \alpha_j, \tag{1}$$

where θ is the causal effect of education on smoking for the relevant margin and α_j denotes SNP-specific direct effects on smoking not mediated by education (e.g. horizontal pleiotropy). Valid instruments satisfy $\alpha_j = 0$.

When treatment effects are heterogeneous and some SNPs are invalid, the proportionality in (1) need not hold uniformly across all j. Our strategy therefore identifies locally valid subsets of SNPs and estimates local causal effects across distinct education margins.

2.2 Local Validity via Two-Stage Clustering

Our empirical procedure enforces validity conditional on instrument-induced education margins. First, SNPs are partitioned into first-stage "clubs" based on similarity in their education associations $\hat{\beta}_{Dj}$ (implemented via hierarchical clustering separately by sign of $\hat{\beta}_{Dj}$). This step groups variants with similar first-stage associations with education (in sign and magnitude).

Second, within each first-stage club, we cluster SNPs by their reduced-form smoking associations and retain the largest internally reduced-form subgroup. Let S_g denote the retained subgroup within first-stage club g. Intuitively, this step operationalizes a plurality-type restriction: within each education club, the subgroup with the largest number of instruments is treated as the locally valid set (i.e., $\alpha_j = 0$ for each SNP_j belonging to that subgroup), while smaller subgroups are allowed to contain pleiotropic or otherwise invalid variants.

2.3 Pairwise LATE Estimation Across Education Margins

After identifying, within each first-stage education margin, the dominant reduced-form subgroup S_g, we estimate causal effects by pairing the retained reduced-form clubs across distinct education margins and pooling the selected (valid) SNPs. For any valid club-pair (g, h), let $S_{gh} = S_g \cup S_h$. We estimate

$$\hat{\beta}_{Yj} = \theta_{gh} \hat{\beta}_{Dj} + u_j, \qquad j \in S_{gh},$$

via a no-intercept regression. The resulting estimator can be written as

$$\hat{\theta}_{gh} = \frac{\sum_{j \in S_{gh}} \hat{\beta}_{Dj} \hat{\beta}_{Yj}}{\sum_{j \in S_{gh}} \hat{\beta}_{Dj}^2}, \tag{2}$$

which is a Wald-type summary-statistic IV estimator. Each θ_{gh} measures how variation in genetically predicted education across the pooled SNPs translates into variation in smoking behavior.

This estimator admits an equivalent weighted-average representation in terms of SNP-specific Wald ratios, with weights proportional to first-stage strength (see Appendix A for derivation).

2.4 IV Assumptions and Interpretation

Education D is measured in years of schooling and is therefore continuous. Our algorithm operates on GWAS summary statistics at the SNP level and therefore treats SNPs as the observational units. The first-stage clustering step partitions the set of instruments into mutually exclusive clubs $\{\mathscr{C}_g\}$, and the reduced-form clustering step retains a mutually exclusive selected subset $S_g \subset \mathscr{C}_g$ within each club.

For interpretation at the individual level, however, genetic instruments are not mutually exclusive: each individual carries a combination of alleles across all SNPs, so all candidate variants potentially shift education simultaneously. We therefore interpret our estimates through a latent-index framework in which instruments shift the latent propensity for education along different margins, rather than through disjoint complier groups defined by single-instrument assignment.

To interpret margin-specific IV estimands, we adopt a latent-index representation in the spirit of Vytlacil (2002) and the marginal treatment effect literature.

Assume a separable latent-index model

$$D = p(\mathbf{Z}) + U,$$

where $\mathbf{Z}$ denotes the vector of genetic variants (SNP allelic dosages) and $p(\mathbf{Z})$ is a scalar index summarizing their joint effect on education. Under the IV independence condition, conditional on GWAS design controls, U is independent of $\mathbf{Z}$. Different SNP clusters correspond to different shifts in $p(\mathbf{Z})$ and therefore index distinct margins of educational variation.

Assumption 1 (Relevance). For each pair (g, h) used in estimation, the pooled instrument set must generate non-negligible first-stage variation in education. In summary-statistics form, this requires

$$\sum_{j \in S_{gh}} \beta_{Dj}^2 > 0,$$

so that the denominator of the Wald estimator is well defined.[2]

This requirement is satisfied in our application because the SNPs entering the hierarchical procedure are selected from variants with strong and statistically well-established associations with education.

Assumption 2 (Independence).

$$\mathbf{Z} \perp\!\!\!\perp \big(\{Y(d) : d \in \mathscr{D}\}, U\big),$$

[2]This condition is the summary-statistics analogue of the standard IV relevance requirement that the instrument set generates nonzero first-stage variation. In a multi-instrument setting, relevance concerns the pooled strength of the instrument vector rather than any single instrument individually.

conditional on the GWAS design controls (e.g. ancestry principal components) and population-structure adjustments and where $\mathscr{D}$ denotes the support of education.

This independence assumption corresponds to the standard Mendelian randomization framework, in which genetic variants are treated as approximately randomly assigned at conception after adjustment for ancestry and population structure.

Assumption 3 (Exclusion / local validity). For SNPs retained in the selected sets, direct effects on smoking are absent:

$$Y(d, \mathbf{Z}) = Y(d).$$

Equivalently, within the selected (locally valid) sets used for a given pairwise comparison, the reduced-form and first-stage associations are approximately proportional, $\beta_{Yj} = \theta_{gh}\,\beta_{Dj}$ for $j \in S_{gh}$, up to sampling noise.

Assumption 4 (Monotonicity and margins). We assume that the instrument-induced index $p(\mathbf{Z})$ can be ordered globally in a meaningful way. That is, for any finite collection of instrument values $\mathbf{Z}_1, \mathbf{Z}_2, \ldots, \mathbf{Z}_K$ such that

$$p(\mathbf{Z}_1) \geq p(\mathbf{Z}_2) \geq \cdots \geq p(\mathbf{Z}_K),$$

it holds for all individuals in the population that

$$D(\mathbf{Z}_1) \geq D(\mathbf{Z}_2) \geq \cdots \geq D(\mathbf{Z}_K).$$

This global monotonicity condition rules out the presence of systematic "defiers," in the sense that increases in the education index never reduce schooling for any individual. Under this assumption, different SNP clusters shift individuals along a common latent ordering of educational propensity, so that pairwise comparisons across clusters identify causal responses along distinct but consistently ordered education margins.

Different cluster pairs index different regions of the education distribution. The hierarchical estimator therefore maps how the causal effect of education on smoking varies across margins, rather than imposing a single homogeneous effect.

3 Methods

This section describes the empirical procedure used to estimate local causal effects of education on smoking behavior using genetic instruments. The method combines hierarchical clustering, plurality-based validity selection, and pairwise Wald estimators across instrument-defined education margins.

3.1 First-Stage Clustering: Education Margins

We first partition SNPs into clusters based on similarity in their education associations.

Dissimilarity matrix. To account for heterogeneous precision across SNP-specific GWAS estimates, we work with standardized first-stage associations (z-scores),[3]

$$z_{Dj} = \frac{\hat{\beta}_{Dj}}{\hat{\sigma}_{Dj}}.$$

We define the pairwise dissimilarity matrix as

$$H^{(D)}_{j,k} = \left| z_{Dj} - z_{Dk} \right|.$$

Clustering is performed separately by sign of $\hat{\beta}_{Dj}$ to avoid mechanically mixing instruments with opposite first-stage directions.

Ward hierarchical clustering. Agglomerative clustering is implemented using Ward linkage (Ward, 1963). For clusters A and B,

[3] These z-scores are standardized GWAS statistics and should not be confused with the instrument vector $\mathbf{Z}$ used in the model.

$$L(A,B) = \frac{|A||B|}{|A|+|B|} \left\| \bar{z}_D(A) - \bar{z}_D(B) \right\|^2,$$

where $|A|$ and $|B|$ denote cluster sizes and $\bar{z}_D(A)$ and $\bar{z}_D(B)$ are the cluster means of the standardized first-stage statistics. Ward linkage merges the pair of clusters that minimizes the increase in within-cluster variance.

Optimal number of clusters. The number of clusters is chosen by maximizing the Calinski–Harabasz index (Caliński and Harabasz, 1974),

$$CH(K) = \frac{B_K/(K-1)}{W_K/(J-K)},$$

where B_K denotes the between-cluster sum of squares and W_K the within-cluster sum of squares under a partition with K clusters, J is the total number of SNPs, and K the number of clusters. The index therefore compares between-cluster dispersion to within-cluster dispersion. Larger values of $CH(K)$ indicate partitions in which clusters are well separated while remaining internally homogeneous, which is consistent with our goal of identifying distinct education margins defined by homogeneous first-stage behavior.

The resulting clusters $\mathscr{C}_g$ represent distinct instrument-induced education margins.

3.2 Reduced-Form Clustering and Validity Selection

Within each first-stage cluster $\mathscr{C}_g$, we repeat the clustering procedure using reduced-form coefficients.

Reduced-form dissimilarity. Within each first-stage club $\mathscr{C}_g$, we standardize reduced-form associations using the within-club mean and standard deviation,

$$z_{Yj}^{(g)} = \frac{\hat{\beta}_{Yj} - \bar{\beta}_{Y,g}}{s_{Y,g}}, \qquad j \in \mathscr{C}_g,$$

where $\bar{\beta}_{Y,g}$ and $s_{Y,g}$ denote the mean and standard deviation of $\hat{\beta}_{Yj}$ within $\mathscr{C}_g$. This within-club standardization centers the reduced-form coefficients and scales them by their dispersion, allowing clustering to focus on relative proportionality patterns rather than level differences across education margins. The dissimilarity matrix is then

$$H_{j,k}^{(Y,g)} = \left| z_{Yj}^{(g)} - z_{Yk}^{(g)} \right|.$$

Hierarchical clustering and the Calinski–Harabasz rule are applied within each g.

Plurality validity rule. Within each first-stage cluster $\mathscr{C}_g$, the reduced-form (RF) clustering step partitions $\mathscr{C}_g$ into RF-subclusters $\{\mathscr{C}_{g\ell}\}_{\ell=1}^{K_g}$. We retain the largest RF-subcluster,

$$S_g = \mathscr{C}_{g\ell^*}, \qquad \ell^* \in \arg\max_{\ell \in \{1,\dots,K_g\}} |\mathscr{C}_{g\ell}|. \tag{3}$$

This dominant subgroup is interpreted as the locally valid instrument set within margin g. All remaining RF-subclusters $\mathscr{C}_{g\ell}$ with $\ell \neq \ell^*$ are discarded. Validity is therefore enforced conditionally on the education margin.

Future extensions could complement this selection step with heterogeneity diagnostics based on summary statistics, such as Cochran's Q statistic used in the Mendelian randomization literature to measure residual dispersion across instruments.[4]

3.3 Pairwise Wald Estimation

After selecting $\{S_g\}_{g=1}^{G}$, we estimate causal effects by pairing reduced-form clubs across education margins. For any pair (g,h) we pool the retained instrument sets $S_{gh} = S_g \cup S_h$ and compute the pairwise Wald estimator $\hat{\theta}_{gh}$ defined in equation (2).

Each estimator $\hat{\theta}_{gh}$ can be interpreted as a Local Average Treatment Effect indexed

[4]In conventional individual-level IV estimation, overidentification tests such as Sargan's rely on regression residuals and cannot be implemented using GWAS summary statistics. Cochran's Q statistic provides an alternative heterogeneity diagnostic that operates directly on instrument-specific summary estimates.

by the paired education margins (g, h). Pooling valid SNP sets across margins combines genetic variation that affects education in different ways and identifies the average causal effect on smoking behavior for individuals whose schooling changes in response to that cross-margin shift. Differences across (g, h) pairs therefore reveal heterogeneity in the causal effect of education on smoking across instrument-defined margins. The procedure does not impose a single global homogeneous effect; instead, it recovers a collection of local causal parameters that map how the education–smoking relationship varies across distinct regions of educational variation.

Figure 1 provides a graphical representation of the hierarchical procedure used to construct locally valid instrument sets conditional on education margins.

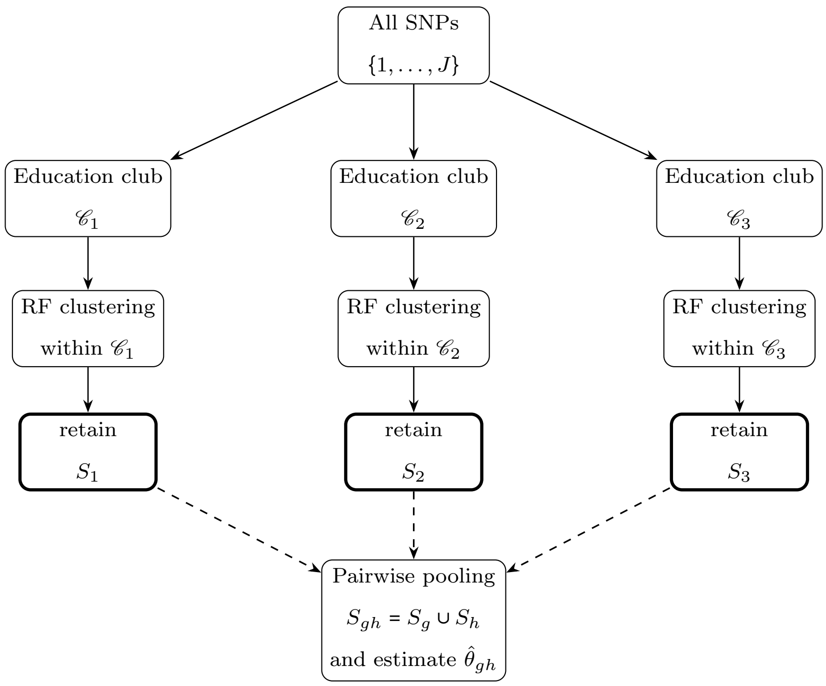

Figure 1: Hierarchical selection of locally valid SNP sets conditional on education margins. SNPs are first partitioned into education clubs $\mathscr{C}_g$ using first-stage associations. Within each C_g, reduced-form clustering is used to retain the dominant subgroup S_g. Pairwise LATEs are estimated by pooling retained sets across margins.

3.4 Bootstrap Inference

To account for clustering uncertainty, we implement a nonparametric bootstrap at the SNP level. Let $\hat{\theta}_{gh}$ denote the pairwise LATE estimator defined in Equation 2. For each bootstrap replication $b = 1, \ldots, B$, SNPs are resampled with replacement from $\{1, \ldots, J\}$, the full clustering and instrument selection procedure is repeated, and the estimator $\hat{\theta}_{gh}^{(b)}$ is recomputed.

Inference is based on the bias-corrected and accelerated (BCa) bootstrap of Efron (1987). We report BCa bootstrap confidence intervals because the estimator depends on a data-driven clustering and instrument selection procedure, which may induce finite-sample bias and skewness in the bootstrap distribution; the BCa correction adjusts for both effects and improves coverage relative to percentile intervals. Define the bias-correction term

$$z_0 = \Phi^{-1}\left(\frac{1}{B}\sum_{b=1}^{B} \mathbb{1}\left(\hat{\theta}_{gh}^{(b)} < \hat{\theta}_{gh}\right)\right),$$

and let $\hat{\theta}_{gh}^{(-j)}$ denote the leave-one-SNP-out jackknife estimator, with mean

$$\bar{\theta}_{\cdot} = \frac{1}{J}\sum_{j=1}^{J} \hat{\theta}_{gh}^{(-j)}.$$

The acceleration parameter is

$$a = \frac{\sum_{j=1}^{J}\left(\bar{\theta}_{\cdot} - \hat{\theta}_{gh}^{(-j)}\right)^3}{6\left[\sum_{j=1}^{J}\left(\bar{\theta}_{\cdot} - \hat{\theta}_{gh}^{(-j)}\right)^2\right]^{3/2}}.$$

Let $z_\alpha = \Phi^{-1}(\alpha)$. The adjusted quantile levels are

$$\alpha_1 = \Phi\left(z_0 + \frac{z_0 + z_{\alpha/2}}{1 - a(z_0 + z_{\alpha/2})}\right), \qquad \alpha_2 = \Phi\left(z_0 + \frac{z_0 + z_{1-\alpha/2}}{1 - a(z_0 + z_{1-\alpha/2})}\right).$$

The $(1-\alpha)$ confidence interval is

$$\left[q_{\alpha_1}, q_{\alpha_2}\right],$$

where q_α denotes the empirical α-quantile of $\{\hat{\theta}_{gh}^{(b)}\}_{b=1}^{B}$.

3.5 Mendelian Randomization

In this subsection we present conventional Mendelian Randomization (MR) estimates as a benchmark for our clustering-based procedure. MR can be viewed as an instrumental variable framework in which genetic variants serve as instruments for an endogenous exposure. Because alleles are randomly assigned at conception, conditional on ancestry, genetic variants are plausibly independent of many environmental confounders. Under the usual IV assumptions — relevance, independence, and exclusion — the association between a variant and the outcome can be interpreted as operating through its effect on the exposure.

MR can be implemented in either a one-sample or a two-sample design. In a one-sample MR, the first stage (variant–exposure association) and the reduced form (variant–outcome association) are estimated within the same dataset of individuals, and the causal effect is obtained via standard two-stage least squares. In a two-sample MR, the first-stage and reduced-form coefficients are estimated in separate genome-wide association studies (GWAS), potentially based on different samples. The causal effect is then constructed by combining the variant-specific first-stage and reduced-form estimates in a Wald-type estimator. Two-sample designs allow researchers to leverage very large GWAS datasets and operate at the level of instrument-specific regression coefficients rather than individual-level data.

In our application, we implement a two-sample MR design using GWAS summary statistics for educational attainment and smoking behavior. The reported SNP effects $\hat{\beta}_{Dj}$ and $\hat{\beta}_{Yj}$ are obtained from large-scale regressions that already adjust for standard covariates such as age, sex, and ancestry principal components. These adjustments are embedded in the GWAS construction and are not re-estimated in our procedure.

Let $\hat{\beta}_{Dj}$ denote the estimated association between SNP j and education (first stage), and $\hat{\beta}_{Yj}$ the estimated association between the same SNP and smoking (reduced form). The SNP-specific Wald ratio is

$$\hat{\theta}_j = \frac{\hat{\beta}_{Yj}}{\hat{\beta}_{Dj}},$$

which represents the causal effect implied by SNP j under the standard IV assumptions.

A central concern in MR is horizontal pleiotropy: genetic variants may affect smoking through pathways other than education. To address this, MR studies frequently invoke the **InSIDE** assumption (*Instrument Strength Independent of Direct Effect*):

$$\mathrm{Cov}(\alpha_j, \beta_{Dj}) = 0,$$

where α_j denotes the direct (pleiotropic) effect of SNP j on smoking not mediated by education. This assumption allows for the instruments to exert a direct effect on the outcome (such in the case of pleiotropy), provided that this direct effect is independent of instrument strength (see also Kolesár et al., 2015, for a discussion of a related assumption).

We implement standard MR estimators that aggregate SNP-specific Wald ratios. The inverse-variance weighted (IVW) estimator corresponds to a weighted no-intercept regression of $\hat{\beta}_{Yj}$ on $\hat{\beta}_{Dj}$, while MR-Egger allows for a nonzero intercept capturing directional pleiotropy:

$$\hat{\beta}_{Yj} = \alpha_0 + \theta\,\hat{\beta}_{Dj} + \varepsilon_j.$$

Here θ is the pooled causal effect[5] and α_0 measures average pleiotropic bias. A statistically significant intercept indicates aggregate violation of the exclusion restriction.

These MR estimators impose a homogeneous-effect structure across SNPs and therefore recover a single pooled causal parameter. They serve as a benchmark against which we compare the heterogeneous LATE estimates obtained from our clustering-based procedure.

[5] By construction, MR-Egger imposes a homogeneous causal parameter across SNPs and therefore recovers a pooled effect rather than margin-specific responses.

4 Empirical Application

4.1 Data

GWAS Summary Statistics

For educational attainment, we use summary statistics from the GWAS of Okbay et al. (2022), based on a meta-analysis of approximately three million individuals of primarily European ancestry.[6] The reported coefficients are standardized per-allele effects on educational attainment, and standard errors are adjusted using LD score regression to account for residual population structure and relatedness.

For smoking behavior, we use summary statistics from Karlsson Linnér et al. (2019), focusing on the "ever smoker" phenotype. This GWAS meta-analysis combines data from the Tobacco and Genetics Consortium (Tobacco and Genetics Consortium, 2010) and the UK Biobank, with a maximum sample size of 518,633 individuals. The phenotype captures smoking participation (ever versus never smoker). As in the educational attainment GWAS, coefficients are standardized per-allele effects and incorporate genomic control adjustments. The summary statistics provided by Karlsson Linnér et al. (2019) include SNPs that pass standard quality-control procedures and a sample-size filter, and are restricted to variants with association p-values below 10^{-5} in the smoking GWAS.

Data Processing and Harmonization

The educational attainment and smoking GWAS both include data from the UK Biobank. The two samples are therefore not fully independent. In two-sample Mendelian Randomization designs, sample overlap can induce finite-sample bias toward the observational association when instruments are weak. In our setting, however, the educational attainment GWAS is based on approximately three million individuals and yields strong first-stage associations for many variants. Given the large sample sizes and instrument strength, any bias induced by partial sample overlap is expected to be limited.

[6] We use the largest non-proprietary set of descriptive statistics, based on an additive GWAS meta-analysis of all discovery cohorts except 23andMe.

We construct our analysis dataset by merging the smoking GWAS summary statistics with the educational attainment GWAS at the SNP level. We begin with all SNPs reported in the "ever smoker" GWAS and match variants to the educational attainment GWAS using unique SNP identifiers. We harmonize effect alleles to ensure consistent orientation across datasets, so that first-stage and reduced-form coefficients correspond to the same effect allele.

After merging and allele alignment, we obtain $33,760$ SNPs for which both first-stage (education) and reduced-form (smoking) associations are available. From this set, we construct our main analysis sample using a standard linkage disequilibrium (LD) clumping procedure. LD refers to the non-random correlation of nearby genetic variants: SNPs that are physically close on the genome tend to be inherited together and therefore capture overlapping genetic information. As a result, even a restricted set of significant SNPs may contain clusters of highly correlated instruments, effectively counting the same underlying source of variation multiple times and overweighting specific genomic regions.

To address this issue, we construct a set of approximately independent instruments using standard LD clumping procedures. Intuitively, clumping groups together SNPs that are highly correlated with each other and retains only one representative variant from each group. In practice, we first identify 'lead' SNPs that are strongly associated with the exposure ($p < 5 \times 10^{-8}$). For each lead SNP, we then assign nearby variants that are both geographically close on the genome (within a 200 kilobase window) and sufficiently correlated with it ($r^2 > 0.2$) to the same cluster, or 'clump'. All non-lead SNPs within each clump are then discarded, leaving a set of variants that are approximately independent of one another. Applying this procedure to the full set of 33,760 SNPs yields a reduced set of 173 instruments.

For comparison, we also consider a specification based on the full set of genome-wide significant SNPs ($N = 5,720$, i.e. all SNPs with $p < 5 \times 10^{-8}$) without LD clumping. This alternative sample allows us to assess the role of correlation across instruments in shaping the results.

4.2 Hierarchical Clustering based results

Figure 2 reports the pairwise LATE estimates obtained from the hierarchical procedure, along with BCa confidence intervals, for the selected subgroup of 173 SNPs. The dominant pattern across panels is a distribution of estimates concentrated near zero but clearly tilted to the left: for the majority of club pairs, the estimated causal effect of education on smoking is negative, consistent with education reducing smoking propensity (see also the corresponding Table B.1 included in Appendix). Relative to the specification reported in Appendix Figure B.1, using the full set of 5,720 SNPs, the distribution obtained from the clumped set of 173 approximately independent SNPs displays a more pronounced mass of negative effects, with many estimates statistically different from zero, while positive estimates are rare. At the same time, the dispersion of estimates across margins remains substantial.

The hierarchical procedure underlying these estimates maps the initial set of 173 SNPs into education clubs based on their first-stage associations. Within each club, reduced-form clustering combined with the plurality rule retains the largest subgroup of instruments that exhibit similar reduced-form behavior, yielding a total of 59 SNPs classified as locally valid instruments. After this selection step, 29 clubs remain for pairwise estimation. Pairwise combinations of these retained sets generate $406 = 29(29-1)/2$ margin-specific LATE estimates. The resulting distribution therefore reflects systematic variation across instrument-defined education margins rather than sampling noise.

While many club pairs cluster around relatively small negative values, a subset of comparisons exhibits larger magnitudes. Only a very limited number of pairwise comparisons yield positive estimates, indicating that the local effect of education need not be uniformly negative across all instrument-induced margins. However, compared to the specification based on the larger set of 5,720 SNPs (Appendix Figure B.1), such positive estimates are less frequent and generally less precisely estimated. This reinforces the interpretation that the dominant relationship is negative, with only isolated margins displaying opposite-signed effects.

One interpretation is that different sets of genetic variants shift educational attainment through distinct mechanisms — for instance, cognitive ability, non-cognitive skills, or behavioral traits — which may in turn have heterogeneous implications for smoking behavior. In particular, some education margins may capture channels through which increased schooling is associated with social environments or peer groups in which smoking is more prevalent, generating positive local effects (see, e.g., Manski, 1993; Sacerdote, 2001, on social interactions and peer effects). Alternatively, these positive estimates may reflect margins where the identifying variation is weaker or more sensitive to remaining pleiotropic pathways. The fact that such estimates are both rare and imprecisely estimated suggests that they do not overturn the overall negative relationship but instead highlight residual heterogeneity across subpopulations.

The BCa confidence intervals reveal substantial variation in the precision of these margin-specific estimates. Compared to the specification based on the full set of 5,720 SNPs (Appendix Figure B.1), the intervals are generally wider. This reflects two complementary factors. First, the reduced number of instruments implies weaker pooled first-stage variation within several club pairs, which mechanically increases estimator variance. Second, because the estimator depends on hierarchical clustering and validity selection, bootstrap resampling can induce greater variability in the composition of the locally valid SNP sets when the number of candidate instruments is smaller. Small perturbations of the bootstrap sample may therefore lead to discrete changes in cluster membership and in the selected subsets, increasing dispersion in the bootstrap distribution. Wide intervals should therefore be interpreted as reflecting weaker identification at specific margins rather than instability of the overall pattern.

Several club pairs nevertheless generate intervals that lie entirely below zero, indicating margins where the education–smoking relationship is both economically meaningful and empirically stable under repeated re-clustering and re-selection of locally valid SNP subsets. Taken together, the results indicate that the heterogeneity observed in Figure 2 is not noise around a single pooled effect. A conventional pooled IV or Mendelian randomization estimator would collapse these margins into a single summary coefficient, implicitly averaging across margins with different levels of identifying strength. The hierarchical procedure instead reveals the internal structure of the instrument set, showing that the overall negative effect masks substantial variation in magnitude and precision across instrument-defined education margins.

Again, a natural benchmark is provided by the specification based on the full set of 5,720 SNPs (Appendix Figure B.1). While that specification benefits from a much larger number of instruments and therefore tighter confidence intervals on average, it also incorporates a dense set of correlated variants. The comparison highlights a trade-off between precision and instrument independence: the clumped set of 173 SNPs yields less precise but more interpretable estimates based on approximately independent sources of variation. Importantly, the qualitative pattern — a predominance of negative effects combined with heterogeneity across margins — remains robust across both specifications.

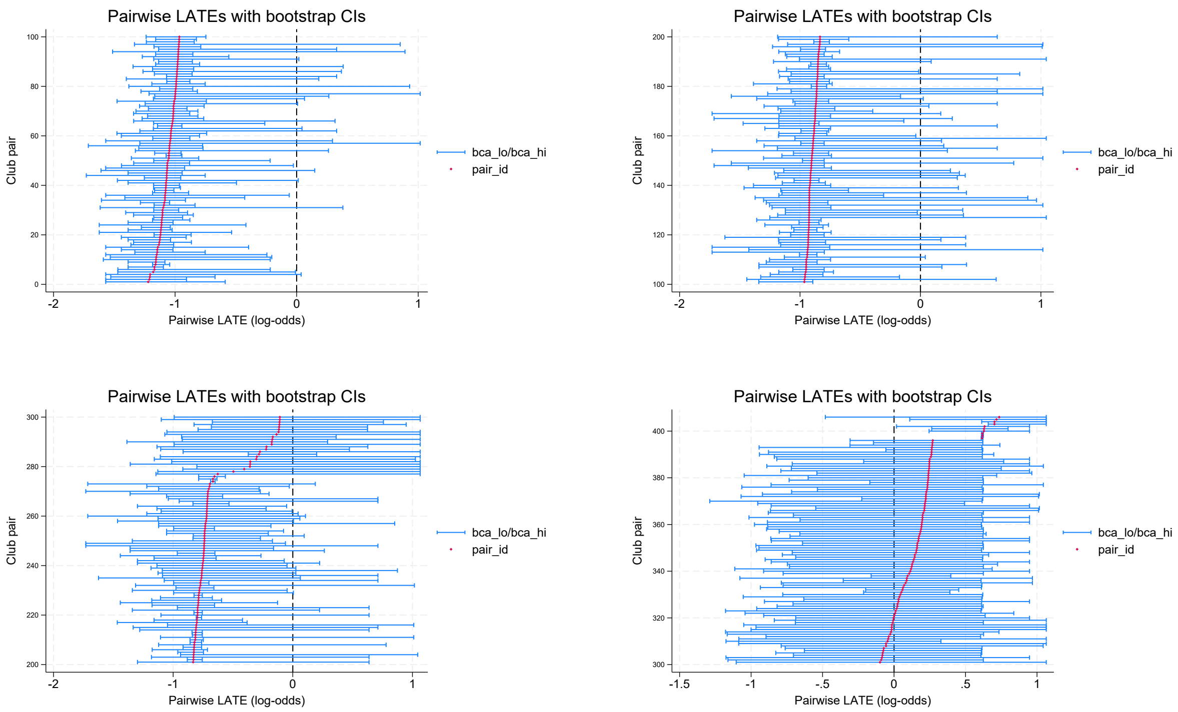

Figure 2: Pairwise LATE plots with BCa CI for the selected subgroup of 173 SNPs.

4.3 Mendelian Randomization based results

Having documented substantial heterogeneity across instrument-defined margins, we now compare these results to conventional Mendelian Randomization estimators that impose a single common causal parameter. We do so using the simple Wald ratio, the inverse-variance weighted (IVW) estimator, and the MR-Egger estimator, alongside the Wald ratio computed using only the subset of SNPs classified as valid by our clustering-based plurality procedure. This comparison clarifies how pooling across all instruments contrasts with restricting attention to locally coherent subsets, while relaxing the exclusion restriction through either the InSIDE assumption or a plurality rule.

Table 1 and Appendix Table B.3 report estimates of the effect of years of education (standardized) on smoking participation using these alternative Mendelian Randomization estimators. Table 1 reports results based on the clumped set of 173 approximately independent SNPs obtained through LD clumping, while Table B.3 uses the full set of SNPs.

Table 1: The effect of education on smoking: MR-Egger, IVW, and Plurality rule using the selected subgroup of 173 SNPs

	(1) Wald ratio	(2) MR Egger	(3) IVW	(4) Plurality
Years of education (std)	-0.488***	0.559***	-0.485***	-0.511***
	(0.054)	(0.178)	(0.054)	(0.092)
N	173	173	173	59

Notes: Standard errors in parentheses. * $p < 0.1$, ** $p < 0.05$, *** $p < 0.01$.

Using the full set of 5,720 SNPs, the estimators deliver markedly different conclusions. The Wald ratio is close to zero and not statistically significant, the IVW estimate is negative and statistically significant, and the MR-Egger estimate is large and positive. While MR-Egger is designed to accommodate directional pleiotropy, it is well known to be sensitive to violations of its identifying assumptions and to weak instrument bias. The magnitude of this estimate, together with its divergence from the IVW result, suggests that allowing for unrestricted pleiotropy without further structure can produce estimates that are difficult to interpret economically. The plurality-based estimate is also positive and statistically significant, but is computed using a subset of 1,012 SNPs selected as locally valid instruments. This dispersion highlights the sensitivity of pooled MR estimators to both instrument heterogeneity and potential violations of the exclusion restriction.

In contrast, when restricting attention to the 173 approximately independent SNPs (Table 1), the estimates become much more aligned. The Wald ratio, IVW, and plurality-based estimates are all negative and of similar magnitude (around -0.5), while the MR-Egger estimate remains positive but substantially smaller and less precise. The plurality procedure selects 59 SNPs in this specification and delivers an estimate close to IVW.

The comparison between the two tables is informative about the role of correlation across genetic instruments. When all SNPs are included, clusters of highly correlated variants can effectively act as multiple copies of the same underlying signal, increasing their influence in pooled estimators and in the plurality selection step. By construction, LD clumping retains only one lead SNP per correlated group, yielding a set of approximately independent instruments. From an econometric perspective, this is closer to a setting in which each instrument contributes distinct variation.

These results illustrate two key points. First, correlation across genetic variants can contribute to instability in pooled MR estimates by effectively overweighting clusters of related instruments. Second, even after accounting for such dependence, instrument selection remains important: the plurality-based approach isolates subsets of instruments that identify coherent local effects rather than imposing a single global parameter. The contrast between the two tables underscores that both instrument dependence and heterogeneity are central to understanding the variation in MR estimates.

5 Conclusion

This paper proposes a hierarchical instrumental-variables framework designed to uncover heterogeneous causal effects in settings with many instruments and potentially invalid exclusion restrictions. Rather than collapsing all instruments into a single pooled estimate, the method treats the instrument set as structurally informative: SNPs are first organized into education margins through hierarchical clustering, then refined through a validity-selection step based on a plurality rule, and finally used to estimate pairwise LATEs. The resulting object is therefore not a single coefficient but a collection of margin-specific causal responses across instrument-defined education margins.

Empirically, the hierarchical estimates reveal a clear pattern: most local effects of education on smoking are negative, consistent with education exerting a protective influence on smoking behavior. At the same time, the magnitude and precision of these effects vary across margins. Some club pairs generate tightly estimated negative effects, while others are more weakly identified. This pattern reflects differences in the strength and internal coherence of the instrument sets associated with each education margin. By revealing this structure, the hierarchical approach provides a richer picture of the education–smoking relationship than conventional pooled IV or Mendelian randomization estimators, which summarize all instruments into a single average effect.

Inference is conducted using bias-corrected and accelerated bootstrap confidence intervals that re-run the full clustering and validity-selection procedure within each bootstrap replication. This approach incorporates uncertainty arising both from sampling variability and from the data-driven classification of instruments.

Our main specification, based on a pruned set of 173 approximately independent genetic instruments, yields a clear and consistent pattern. Despite the substantially smaller number of SNPs relative to the full set of 5,720 variants reported in the Appendix, the distribution of margin-specific estimates remains tilted toward negative effects and continues to display heterogeneity across education margins. The reduction in the number of instruments leads to wider confidence intervals for some club pairs, reflecting weaker identification in specific margins. However, this loss in precision does not alter the overall pattern of results. The comparison therefore indicates that our findings are not driven by the large number of SNPs in the alternative specification, but instead reflect robust patterns across instrument sets.

More broadly, the framework applies to policy environments with multiple instruments that shift treatment along distinct margins of compliance. In such settings, conventional IV estimators aggregate across heterogeneous margins and may obscure meaningful variation in causal responses. Examples include institutional settings where treatment assignment is influenced by different judges, caseworkers, or administrative rules, policy environments where eligibility thresholds generate multiple instruments, or geographic variation in program exposure across regions. By identifying locally coherent instrument subsets and estimating margin-specific effects, the hierarchical approach provides a way to recover richer treatment-effect heterogeneity, consistent with the broader LATE and marginal treatment effect literature (Imbens and Angrist, 1994; Heckman and Vytlacil, 2005).

Several extensions remain open. Future work could explore alternative clustering metrics, adaptive validity-selection rules, or Bayesian approaches that jointly model clustering and causal estimation. Further theoretical work on inference after data-driven clustering and on weak identification within specific margins would also deepen understanding of the large-sample behavior of hierarchical IV estimators. Taken together, our findings underscore the importance of accounting for heterogeneity across instrument-defined margins when evaluating the causal effects of education on smoking behavior.

References

Alvarez, A., and R. Toneto. 2024. The interpretation of 2SLS with a continuous instrument: A weighted LATE representation. Economics Letters, 237(111658).

Angrist, J., G. Imbens, and D. Rubin. 1996. Identification of Causal Effects using Instrumental Variables. Journal of the American Statistical Association, 91(434): 444–472 (with discussion).

Apfel, N., H. Farbmacher, G. Groh, M. Huber, and H. Langen. 2023. Detecting Grouped Local Average Treatment Effects and Selecting True Instruments With an Application to Estimating the Effect of Prison on Recidivism. working paper, Cornell University, https://doi.org/10.48550/arXiv.2207.04481.

Bowden, J., G. D. Smith, P. Haycock, and S. Burgess. 2016. Consistent Estimation in Mendelian Randomization with Some Invalid Instruments Using a Weighted Median Estimator. Genetic Epidemiology, 40(4): 304–314.

Burgess, S., C. N. Foley, E. Allara, J. R. Staley, and J. M. Howson. 2020. A robust and efficient method for Mendelian randomization with hundreds of genetic variants. Nature communications, 11(1): 376.

Clark, D., and H. Royer. 2013. The effect of education on adult mortality and health: Evidence from Britain. American Economic Review, 103(6): 2087–2120.

Davey Smith, G., and G. Hemani. 2014. Mendelian randomization: genetic anchors for causal inference in epidemiological studies. Human Molecular Genetics, 23(R1): R89–R98.

Davies, N. M., M. Dickson, G. Davey Smith, G. J. Van Den Berg, and F. Windmeijer. 2018. The causal effects of education on health outcomes in the UK Biobank. Nature Human Behaviour, 2(2): 117–125.

Efron, B. 1987. Better Bootstrap Confidence Intervals. Journal of the American Statistical Association, 82(397): 171–185.

Gage, S. H., J. Bowden, G. Davey Smith, and M. R. Munafò. 2018. Investigating causality in associations between education and smoking: a two-sample Mendelian randomization study. International journal of epidemiology, 47(4): 1131–1140.

Hartwig, F. P., G. Davey Smith, and J. Bowden. 2017. Robust inference in summary data Mendelian randomization via the zero modal pleiotropy assumption. International journal of epidemiology, 46(6): 1985–1998.

Heckman, J. J., and E. Vytlacil. 2005. Structural Equations, Treatment Effects, and Econometric Policy Evaluation. Econometrica, 73(3): 669–738.

Imbens, G. W., and J. Angrist. 1994. Identification and Estimation of Local Average Treatment Effects. Econometrica, 62(2): 467–475.

Kang, H., A. Zhang, T. Cai, and D. Small. 2016. Instrumental variables estimation with some invalid instruments and its application to Mendelian randomization. Journal of the American Statistical Association, 111(513): 132–144.

Karlsson Linnér, R., P. Biroli, E. Kong, S. F. W. Meddens, R. Wedow, M. A. Fontana, M. Lebreton, S. P. Tino, A. Abdellaoui, A. R. Hammerschlag, et al. 2019. Genome-wide association analyses of risk tolerance and risky behaviors in over 1 million individuals identify hundreds of loci and shared genetic influences. Nature Genetics, 51(2): 245–257.

Kolesár, M., R. Chetty, J. Friedman, E. Glaeser, and I. Shapiro. 2015. Identification and Inference With Many Invalid Instruments. Journal of Business & Economic Statistics, 33(4): 474–484.

Manski, C. F. 1993. Identification of Endogenous Social Effects: The Reflection Problem. Review of Economic Studies, 60(3): 531–542.

Mogstad, M., and A. Torgovitsky. 2024. Instrumental variables with unobserved heterogeneity in treatment effects. In Handbook of Labor Economics. Vol. 5, , ed. O. Ashenfelter and D. Card, 1–114. Elsevier.

Mogstad, M., A. Torgovitsky, and C. R. Walters. 2021. The causal interpretation of two-stage least squares with multiple instrumental variables. American Economic Review, 111(11): 3663–3698.

Okbay, A., J. P. Beauchamp, M. A. Fontana, J. J. Lee, T. H. Pers, C. A. Rietveld, P. Turley, G.-B. Chen, V. Emilsson, S. F. W. Meddens, et al. 2016. Genome-wide association study identifies 74 loci associated with educational attainment. Nature, 533(7604): 539–542.

Okbay, A., Y. Wu, N. Wang, H. Jayashankar, M. Bennett, S. M. Nehzati, J. Sidorenko, H. Kweon, G. Goldman, T. Gjorgjieva, et al. 2022. Polygenic prediction of educational attainment within and between families from genome-wide association analyses in 3 million individuals. Nature Genetics, 54(4): 437–449.

Sacerdote, B. 2001. Peer Effects with Random Assignment: Results for Dartmouth Roommates. Quarterly Journal of Economics, 116(2): 681–704.

Sanderson, E., G. Davey Smith, J. Bowden, and M. R. Munafò. 2019. Mendelian randomisation analysis of the effect of educational attainment and cognitive ability on smoking behaviour. Nature Communications, 10(1): 2949.

Tobacco and Genetics Consortium. 2010. Genome-wide meta-analyses identify multiple loci associated with smoking behavior. Nature Genetics, 42(5): 441–447.

Vytlacil, E. 2002. Independence, Monotonicity, and Latent Index Models: An Equivalence Result. Econometrica, 70(1): 331–341.

Ward, J. H. J. 1963. Hierarchical Grouping to Optimize an Objective Function. Journal of the American Statistical Association, 58(301): 236–244.

Windmeijer, F., H. Farbmacher, N. Davies, and G. Davey Smith. 2019. On the use of the lasso for instrumental variables estimation with some invalid instruments. Journal of the American Statistical Association, 114(527): 1339–1350.

Appendix A Derivation of the Pairwise Wald Estimator

Fix a given pair of education margins (g, h) and consider the pooled set of SNPs $S_{gh} = S_g \cup S_h$ selected by the hierarchical procedure. Estimation is based on the no-intercept regression across SNP-specific summary statistics

$$\hat{\beta}_{Yj} = \theta_{gh}\hat{\beta}_{Dj} + u_j, \qquad j \in S_{gh}.$$

The ordinary least squares estimator minimizes the sum of squared residuals

$$\sum_{j \in S_{gh}} \left(\hat{\beta}_{Yj} - \theta_{gh}\hat{\beta}_{Dj}\right)^2.$$

Taking the first-order condition with respect to θ_{gh} yields

$$\sum_{j \in S_{gh}} \hat{\beta}_{Dj}\left(\hat{\beta}_{Yj} - \theta_{gh}\hat{\beta}_{Dj}\right) = 0.$$

Rearranging gives

$$\sum_{j \in S_{gh}} \hat{\beta}_{Dj}\hat{\beta}_{Yj} = \theta_{gh} \sum_{j \in S_{gh}} \hat{\beta}_{Dj}^2,$$

and therefore

$$\hat{\theta}_{gh} = \frac{\sum_{j \in S_{gh}} \hat{\beta}_{Dj}\hat{\beta}_{Yj}}{\sum_{j \in S_{gh}} \hat{\beta}_{Dj}^2}.$$

Each SNP $j \in S_{gh}$ also admits a Wald ratio estimate

$$\hat{\theta}_j = \frac{\hat{\beta}_{Yj}}{\hat{\beta}_{Dj}}.$$

Substituting $\hat{\beta}_{Yj} = \hat{\theta}_j\hat{\beta}_{Dj}$ into the numerator shows that the pooled estimator can be written as

$$\hat{\theta}_{gh} = \frac{\sum_{j \in S_{gh}} \hat{\theta}_j\hat{\beta}_{Dj}^2}{\sum_{j \in S_{gh}} \hat{\beta}_{Dj}^2}.$$

Hence, conditional on the chosen pair of education margins, the estimator is a weighted average of SNP-specific Wald ratios, where weights are proportional to squared first-stage strength. Stronger instruments therefore receive greater influence in the pooled estimate.

Appendix B Pairwise LATE estimates

Table B.1 reports all pairwise education-margin-specific LATE estimates, $\hat{\theta}_{gh}$, derived from our hierarchical approach, along with percentile bootstrap confidence intervals. The bootstrap procedure incorporates the full clustering and valid-set selection steps in each replication.

Table B.1: Results by club pair, using the selected subgroup of 173 SNPs, with point estimate ($\hat{\theta}_{gh}$) and Bias Corrected and Accelerated Bootstrap CI. Significance stars: $^{*}p < 0.1$, $^{**}p < 0.05$, $^{***}p < 0.01$ (two-sided; p-values inferred from 95% interval assuming normality).

Club1	**Club2**	**Label**	$\hat{\theta}_{gh}$	**bca_lo**	**bca_hi**
1	2	Club_1_2	-1.155^{***}	-1.533	-0.204
1	3	Club_1_3	-1.180^{***}	-1.471	-0.010
1	4	Club_1_4	-1.170^{***}	-1.471	-0.217
1	5	Club_1_5	-1.157^{***}	-1.590	-0.217
1	6	Club_1_6	-1.072^{***}	-1.475	0.013
1	7	Club_1_7	-1.097^{**}	-1.616	0.380
1	9	Club_1_9	-1.064^{***}	-1.441	-0.027
1	10	Club_1_10	-0.923	-1.373	0.891
1	13	Club_1_13	0.119	-1.114	0.686
1	14	Club_1_14	0.081	-0.789	0.968
1	15	Club_1_15	-0.802^{***}	-1.467	-0.382
1	18	Club_1_18	-0.973	-1.514	0.891
1	20	Club_1_20	-1.103^{***}	-1.406	-0.897
1	21	Club_1_21	-0.992^{*}	-1.380	0.930
1	22	Club_1_22	-1.221^{***}	-1.570	-0.587
1	23	Club_1_23	-0.905	-1.570	0.774
1	24	Club_1_24	-1.212^{***}	-1.570	-0.906
1	25	Club_1_25	-1.066^{**}	-1.609	0.149
1	26	Club_1_26	-1.082^{***}	-1.570	-0.061

Continued on next page

Club1	Club2	Label	$\hat{\theta}_{gh}$	bca_lo	bca_hi
1	27	Club_1_27	-1.142^{***}	-1.570	-0.395
1	28	Club_1_28	-1.205^{***}	-1.570	0.037
1	29	Club_1_29	-1.207^{***}	-1.529	-0.671
1	30	Club_1_30	-0.305	-1.158	1.025
1	31	Club_1_31	-1.151^{***}	-1.570	-0.245
1	34	Club_1_34	0.127	-0.746	0.724
1	35	Club_1_35	0.090	-1.078	0.968
1	36	Club_1_36	-1.040^{**}	-1.570	0.295
1	37	Club_1_37	-0.863^{**}	-1.570	-0.166
2	3	Club_2_3	-1.013^{***}	-1.219	-0.902
2	4	Club_2_4	-0.990^{***}	-1.068	-0.878
2	5	Club_2_5	-0.984^{**}	-1.264	0.368
2	6	Club_2_6	-0.915^{***}	-1.050	-0.842
2	7	Club_2_7	-0.928^{***}	-1.051	-0.860
2	9	Club_2_9	-0.916^{***}	-1.147	-0.790
2	10	Club_2_10	-0.830^{***}	-0.882	-0.757
2	13	Club_2_13	0.263	-0.878	0.617
2	14	Club_2_14	0.235	-0.169	0.625
2	15	Club_2_15	-0.719^{**}	-1.101	-0.006
2	18	Club_2_18	-0.856^{*}	-1.099	0.637
2	20	Club_2_20	-0.969^{***}	-1.174	-0.789
2	21	Club_2_21	-0.852^{***}	-0.927	-0.762
2	22	Club_2_22	-1.109^{***}	-1.185	-0.878
2	23	Club_2_23	-0.762^{*}	-1.089	0.711
2	24	Club_2_24	-1.080^{***}	-1.185	-0.889
2	25	Club_2_25	-0.892^{***}	-0.993	-0.800
2	26	Club_2_26	-0.912^{**}	-1.184	0.372
2	27	Club_2_27	-0.982^{***}	-1.185	-0.847
2	28	Club_2_28	-1.037^{***}	-1.184	-0.878

Continued on next page

Club1	Club2	Label	$\hat{\theta}_{gh}$	bca_lo	bca_hi
2	29	Club_2_29	-1.117^{***}	-1.386	-1.024
2	30	Club_2_30	-0.016	-0.966	1.065
2	31	Club_2_31	-0.973^{***}	-1.135	0.329
2	34	Club_2_34	0.269	-0.144	0.621
2	35	Club_2_35	0.247	-0.712	0.948
2	36	Club_2_36	-0.925^{**}	-1.185	0.357
2	37	Club_2_37	-0.755^{**}	-1.185	0.026
3	4	Club_3_4	-1.027^{***}	-1.144	-0.944
3	5	Club_3_5	-1.020^{**}	-1.341	0.316
3	6	Club_3_6	-0.948^{***}	-1.280	-0.858
3	7	Club_3_7	-0.964^{***}	-1.342	-0.894
3	9	Club_3_9	-0.948^{***}	-1.253	-0.747
3	10	Club_3_10	-0.851^{***}	-0.911	-0.781
3	13	Club_3_13	0.216	-0.953	0.493
3	14	Club_3_14	0.185	-0.803	0.625
3	15	Club_3_15	-0.738^{**}	-1.341	-0.170
3	18	Club_3_18	-0.882^{*}	-1.175	0.637
3	20	Club_3_20	-0.996^{***}	-1.280	-0.816
3	21	Club_3_21	-0.883^{***}	-0.992	-0.762
3	22	Club_3_22	-1.129^{***}	-1.341	-0.866
3	23	Club_3_23	-0.796^{**}	-1.341	0.224
3	24	Club_3_24	-1.104^{***}	-1.341	-0.850
3	25	Club_3_25	-0.930^{***}	-1.078	-0.800
3	26	Club_3_26	-0.949^{**}	-1.341	0.178
3	27	Club_3_27	-1.014^{***}	-1.341	-0.879
3	28	Club_3_28	-1.069^{***}	-1.253	-0.953
3	29	Club_3_29	-1.132^{***}	-1.364	-1.012
3	30	Club_3_30	-0.108	-0.991	1.065
3	31	Club_3_31	-1.009^{***}	-1.246	0.008

Continued on next page

Club1	Club2	Label	$\hat{\theta}_{gh}$	bca_lo	bca_hi
3	34	Club_3_34	0.222	-0.226	0.621
3	35	Club_3_35	0.195	-0.886	0.948
3	36	Club_3_36	-0.949^{**}	-1.341	0.382
3	37	Club_3_37	-0.781^{**}	-1.341	-0.047
4	5	Club_4_5	-0.998^{*}	-1.214	1.016
4	6	Club_4_6	-0.925^{***}	-1.008	-0.842
4	7	Club_4_7	-0.940^{***}	-1.005	-0.860
4	9	Club_4_9	-0.926^{***}	-1.070	-0.809
4	10	Club_4_10	-0.835^{***}	-0.886	-0.757
4	13	Club_4_13	0.265	-0.944	0.615
4	14	Club_4_14	0.238	-0.734	0.625
4	15	Club_4_15	-0.722^{**}	-1.127	0.059
4	18	Club_4_18	-0.863^{**}	-1.075	0.637
4	20	Club_4_20	-0.979^{***}	-1.160	-0.798
4	21	Club_4_21	-0.860^{***}	-0.907	-0.779
4	22	Club_4_22	-1.120^{***}	-1.173	-0.868
4	23	Club_4_23	-0.769^{*}	-1.075	0.711
4	24	Club_4_24	-1.091^{***}	-1.173	-0.836
4	25	Club_4_25	-0.903^{***}	-0.980	-0.800
4	26	Club_4_26	-0.924^{**}	-1.122	0.351
4	27	Club_4_27	-0.994^{***}	-1.127	-0.854
4	28	Club_4_28	-1.051^{***}	-1.074	-0.944
4	29	Club_4_29	-1.125^{***}	-1.386	-1.037
4	30	Club_4_30	-0.015	-1.051	1.065
4	31	Club_4_31	-0.986^{***}	-1.070	0.329
4	34	Club_4_34	0.271	-0.307	0.621
4	35	Club_4_35	0.250	-0.820	0.948
4	36	Club_4_36	-0.932^{**}	-1.161	0.376
4	37	Club_4_37	-0.761^{***}	-1.127	0.025

Continued on next page

Club1	Club2	Label	$\hat{\theta}_{gh}$	bca_lo	bca_hi
5	6	Club_5_6	−0.923	-1.303	0.964
5	7	Club_5_7	−0.937	-1.425	1.016
5	9	Club_5_9	−0.924	-1.253	1.016
5	10	Club_5_10	−0.836	-1.103	1.016
5	13	Club_5_13	0.242	-0.539	0.964
5	14	Club_5_14	0.213	-0.547	1.016
5	15	Club_5_15	−0.725*	-1.465	0.006
5	18	Club_5_18	−0.863	-1.269	1.016
5	20	Club_5_20	−0.975***	-1.270	-0.558
5	21	Club_5_21	−0.860	-1.191	1.016
5	22	Club_5_22	−1.112***	-1.624	-0.417
5	23	Club_5_23	−0.772	-1.314	1.016
5	24	Club_5_24	−1.083***	-1.413	-0.427
5	25	Club_5_25	−0.902	-1.303	1.016
5	26	Club_5_26	−0.922**	-1.465	0.314
5	27	Club_5_27	−0.989**	-1.401	0.182
5	28	Club_5_28	−1.042*	-1.290	1.016
5	29	Club_5_29	−1.118***	-1.624	-0.535
5	30	Club_5_30	−0.056	-0.789	1.043
5	31	Club_5_31	−0.981**	-1.346	0.383
5	34	Club_5_34	0.248	-0.212	0.767
5	35	Club_5_35	0.224	-0.920	1.016
5	36	Club_5_36	−0.931*	-1.624	0.376
5	37	Club_5_37	−0.763*	-1.624	0.063
6	7	Club_6_7	−0.879***	-1.473	-0.842
6	9	Club_6_9	−0.874***	-1.175	-0.747
6	10	Club_6_10	−0.812***	-0.842	-0.757
6	13	Club_6_13	0.192	-0.883	0.614
6	14	Club_6_14	0.161	-0.945	0.625

Continued on next page

Club1	Club2	Label	$\hat{\theta}_{gh}$	bca_lo	bca_hi
6	15	Club_6_15	-0.711^{**}	-1.360	-0.199
6	18	Club_6_18	-0.830^{*}	-1.181	0.637
6	20	Club_6_20	-0.923^{***}	-1.280	-0.768
6	21	Club_6_21	-0.822^{***}	-0.858	-0.762
6	22	Club_6_22	-1.051^{***}	-1.360	-0.806
6	23	Club_6_23	-0.743^{*}	-1.360	0.264
6	24	Club_6_24	-1.017^{***}	-1.271	-0.764
6	25	Club_6_25	-0.847^{***}	-1.122	-0.800
6	26	Club_6_26	-0.865^{**}	-1.360	0.023
6	27	Club_6_27	-0.925^{***}	-1.360	-0.825
6	28	Club_6_28	-0.967^{***}	-1.236	-0.842
6	29	Club_6_29	-1.068^{***}	-1.386	-0.942
6	30	Club_6_30	-0.119	-1.052	1.065
6	31	Club_6_31	-0.912^{**}	-1.212	0.323
6	34	Club_6_34	0.198	-0.657	0.621
6	35	Club_6_35	0.170	-0.858	0.948
6	36	Club_6_36	-0.891^{**}	-1.360	0.175
6	37	Club_6_37	-0.742^{**}	-1.360	-0.161
7	9	Club_7_9	-0.882^{***}	-1.292	-0.747
7	10	Club_7_10	-0.814^{***}	-0.839	-0.757
7	13	Club_7_13	0.233	-1.065	0.616
7	14	Club_7_14	0.205	-0.880	0.625
7	15	Club_7_15	-0.708^{*}	-1.730	-0.272
7	18	Club_7_18	-0.833^{*}	-1.298	0.637
7	20	Club_7_20	-0.934^{***}	-1.730	-0.753
7	21	Club_7_21	-0.825^{***}	-0.917	-0.762
7	22	Club_7_22	-1.069^{***}	-1.730	-0.752
7	23	Club_7_23	-0.741	-1.730	0.711
7	24	Club_7_24	-1.035^{***}	-1.478	-0.740

Continued on next page

Club1	Club2	Label	$\hat{\theta}_{gh}$	bca_lo	bca_hi
7	25	Club_7_25	-0.854^{***}	-1.171	-0.800
7	26	Club_7_26	-0.874^{*}	-1.730	0.169
7	27	Club_7_27	-0.938^{***}	-1.730	-0.798
7	28	Club_7_28	-0.984^{***}	-1.170	-0.860
7	29	Club_7_29	-1.083^{***}	-1.606	-0.914
7	30	Club_7_30	-0.056	-1.087	1.065
7	31	Club_7_31	-0.925	-1.251	1.044
7	34	Club_7_34	0.239	-0.601	0.621
7	35	Club_7_35	0.215	-0.860	0.948
7	36	Club_7_36	-0.898^{*}	-1.730	0.223
7	37	Club_7_37	-0.740^{*}	-1.730	-0.062
9	10	Club_9_10	-0.816^{***}	-0.859	-0.748
9	13	Club_9_13	0.157	-0.962	0.612
9	14	Club_9_14	0.124	-0.731	0.625
9	15	Club_9_15	-0.717^{**}	-1.299	-0.052
9	18	Club_9_18	-0.834^{*}	-1.186	0.637
9	20	Club_9_20	-0.924^{***}	-1.233	-0.744
9	21	Club_9_21	-0.827^{***}	-0.961	-0.747
9	22	Club_9_22	-1.046^{***}	-1.299	-0.770
9	23	Club_9_23	-0.752^{*}	-1.299	0.225
9	24	Club_9_24	-1.013^{***}	-1.292	-0.761
9	25	Club_9_25	-0.853^{***}	-1.112	-0.747
9	26	Club_9_26	-0.870^{**}	-1.299	0.070
9	27	Club_9_27	-0.926^{***}	-1.292	-0.764
9	28	Club_9_28	-0.965^{***}	-1.238	-0.747
9	29	Club_9_29	-1.063^{***}	-1.340	-0.881
9	30	Club_9_30	-0.171	-0.924	1.065
9	31	Club_9_31	-0.913^{**}	-1.203	0.306
9	34	Club_9_34	0.163	-0.640	0.621

Continued on next page

Club1	Club2	Label	$\hat{\theta}_{gh}$	bca_lo	bca_hi
9	35	Club_9_35	0.133	-0.859	0.948
9	36	Club_9_36	-0.892^{**}	-1.299	0.194
9	37	Club_9_37	-0.749^{**}	-1.299	-0.072
10	13	Club_10_13	-0.079	-0.827	0.614
10	14	Club_10_14	-0.116	-0.792	0.625
10	15	Club_10_15	-0.716^{***}	-0.834	-0.533
10	18	Club_10_18	-0.795^{*}	-0.965	0.637
10	20	Club_10_20	-0.848^{***}	-1.110	-0.733
10	21	Club_10_21	-0.786^{***}	-0.826	-0.757
10	22	Club_10_22	-0.932^{***}	-1.175	-0.788
10	23	Club_10_23	-0.738^{***}	-0.832	0.095
10	24	Club_10_24	-0.901^{***}	-1.150	-0.739
10	25	Club_10_25	-0.796^{***}	-0.826	-0.757
10	26	Club_10_26	-0.806	-1.047	1.011
10	27	Club_10_27	-0.841^{***}	-0.996	-0.788
10	28	Club_10_28	-0.860^{***}	-1.087	-0.757
10	29	Club_10_29	-0.958^{***}	-1.247	-0.809
10	30	Club_10_30	-0.406	-0.919	1.065
10	31	Club_10_31	-0.829	-0.938	1.044
10	34	Club_10_34	-0.072	-0.762	0.616
10	35	Club_10_35	-0.112	-0.826	0.948
10	36	Club_10_36	-0.834^{***}	-1.179	-0.595
10	37	Club_10_37	-0.738^{***}	-0.834	-0.270
13	14	Club_13_14	0.618^{***}	0.611	0.625
13	15	Club_13_15	-0.081	-0.704	0.608
13	18	Club_13_18	0.038	-1.055	0.617
13	20	Club_13_20	0.088	-0.355	0.609
13	21	Club_13_21	0.138	-0.902	0.619
13	22	Club_13_22	-0.045	-1.175	0.328

Continued on next page

Club1	Club2	Label	$\hat{\theta}_{gh}$	bca_lo	bca_hi
13	23	Club_13_23	0.175	-0.728	0.622
13	24	Club_13_24	0.063	-0.935	0.611
13	25	Club_13_25	0.258	-0.838	0.617
13	26	Club_13_26	0.240	-1.048	0.718
13	27	Club_13_27	0.193	-0.976	0.611
13	28	Club_13_28	0.219	-1.289	0.616
13	29	Club_13_29	−0.176	-1.386	0.291
13	30	Club_13_30	0.703^{***}	0.613	1.065
13	31	Club_13_31	0.262	-0.941	0.698
13	34	Club_13_34	0.616^{***}	0.610	0.622
13	35	Club_13_35	0.629^{***}	0.245	0.948
13	36	Club_13_36	0.012	-1.179	0.608
13	37	Club_13_37	0.025	-0.707	0.612
14	15	Club_14_15	−0.114	-0.680	0.625
14	18	Club_14_18	0.002	-0.912	0.637
14	20	Club_14_20	0.052	-0.213	0.391
14	21	Club_14_21	0.106	-0.776	0.625
14	22	Club_14_22	−0.090	-1.162	0.625
14	23	Club_14_23	0.146	-0.781	0.662
14	24	Club_14_24	0.023	-0.818	0.623
14	25	Club_14_25	0.231	-0.536	0.625
14	26	Club_14_26	0.212	-0.865	1.011
14	27	Club_14_27	0.162	-0.966	0.625
14	28	Club_14_28	0.189	-0.891	0.625
14	29	Club_14_29	−0.223	-1.104	0.473
14	30	Club_14_30	0.717^{***}	0.110	1.065
14	31	Club_14_31	0.235	-0.860	1.044
14	34	Club_14_34	0.619^{***}	0.612	0.625
14	35	Club_14_35	0.634^{***}	0.017	0.948

Continued on next page

Club1	Club2	Label	$\hat{\theta}_{gh}$	bca_lo	bca_hi
14	36	Club_14_36	−0.027	-1.167	0.626
14	37	Club_14_37	−0.009	-0.690	0.625
15	18	Club_15_18	−0.711***	-1.055	-0.586
15	20	Club_15_20	−0.748***	-1.160	-0.641
15	21	Club_15_21	−0.696**	-1.220	-0.029
15	22	Club_15_22	−0.826***	-1.175	-0.713
15	23	Club_15_23	−0.655***	-0.787	-0.563
15	24	Club_15_24	−0.791***	-1.177	-0.654
15	25	Club_15_25	−0.693	-1.714	0.188
15	26	Club_15_26	−0.702***	-1.122	-0.281
15	27	Club_15_27	−0.733***	-0.996	-0.655
15	28	Club_15_28	−0.745**	-1.442	-0.266
15	29	Club_15_29	−0.860***	-1.386	-0.733
15	30	Club_15_30	−0.359	-0.802	1.065
15	31	Club_15_31	−0.718***	-1.135	-0.223
15	34	Club_15_34	−0.075	-0.627	0.611
15	35	Club_15_35	−0.111	-0.672	0.757
15	36	Club_15_36	−0.744***	-0.965	-0.651
15	37	Club_15_37	−0.667***	-0.787	-0.634
18	20	Club_18_20	−0.873***	-1.160	-0.396
18	21	Club_18_21	−0.796*	-1.102	0.637
18	22	Club_18_22	−0.975***	-1.175	0.019
18	23	Club_18_23	−0.736***	-1.055	-0.077
18	24	Club_18_24	−0.941***	-1.130	0.040
18	25	Club_18_25	−0.810*	-1.279	0.637
18	26	Club_18_26	−0.824*	-1.122	0.780
18	27	Club_18_27	−0.868**	-1.042	0.637
18	28	Club_18_28	−0.894*	-1.188	0.637
18	29	Club_18_29	−1.000***	-1.167	0.265

Continued on next page

Club1	Club2	Label	$\hat{\theta}_{gh}$	bca_lo	bca_hi
18	30	Club_18_30	-0.300	-1.107	1.065
18	31	Club_18_31	-0.854^{*}	-1.074	0.824
18	34	Club_18_34	0.045	-0.779	0.621
18	35	Club_18_35	0.008	-1.042	0.838
18	36	Club_18_36	-0.853^{***}	-1.179	-0.015
18	37	Club_18_37	-0.737^{***}	-1.055	-0.205
20	21	Club_20_21	-0.873^{***}	-1.183	-0.711
20	22	Club_20_22	-1.078^{***}	-1.169	-1.010
20	23	Club_20_23	-0.801^{***}	-1.160	-0.420
20	24	Club_20_24	-1.050^{***}	-1.168	-0.951
20	25	Club_20_25	-0.907^{***}	-1.429	-0.740
20	26	Club_20_26	-0.922^{***}	-1.160	-0.598
20	27	Club_20_27	-0.974^{***}	-1.160	-0.854
20	28	Club_20_28	-1.013^{***}	-1.322	-0.812
20	29	Club_20_29	-1.089^{***}	-1.285	-1.045
20	30	Club_20_30	-0.282^{*}	-0.372	0.200
20	31	Club_20_31	-0.966^{***}	-1.160	-0.824
20	34	Club_20_34	0.095	-0.160	0.397
20	35	Club_20_35	0.059	-0.199	0.453
20	36	Club_20_36	-0.929^{***}	-1.171	-0.742
20	37	Club_20_37	-0.787^{***}	-1.106	-0.673
21	22	Club_21_22	-0.991^{***}	-1.191	-0.752
21	23	Club_21_23	-0.714^{*}	-0.949	0.711
21	24	Club_21_24	-0.953^{***}	-1.177	-0.723
21	25	Club_21_25	-0.798^{***}	-0.807	-0.762
21	26	Club_21_26	-0.814	-1.106	1.011
21	27	Club_21_27	-0.866^{***}	-1.059	-0.762
21	28	Club_21_28	-0.898^{***}	-1.054	-0.762
21	29	Club_21_29	-1.016^{***}	-1.226	-0.812

Continued on next page

Club1	Club2	Label	$\hat{\theta}_{gh}$	bca_lo	bca_hi
21	30	Club_21_30	-0.176	-0.993	1.065
21	31	Club_21_31	-0.850	-1.005	1.044
21	34	Club_21_34	0.145	-0.688	0.621
21	35	Club_21_35	0.114	-0.912	0.948
21	36	Club_21_36	-0.850^{**}	-1.220	0.089
21	37	Club_21_37	-0.720^{**}	-1.220	0.044
22	23	Club_22_23	-0.923^{***}	-1.175	-0.306
22	24	Club_22_24	-1.161^{***}	-1.185	-1.044
22	25	Club_22_25	-1.046^{***}	-1.714	-0.773
22	26	Club_22_26	-1.058^{***}	-1.175	-0.218
22	27	Club_22_27	-1.103^{***}	-1.175	-0.970
22	28	Club_22_28	-1.147^{***}	-1.331	-0.752
22	29	Club_22_29	-1.170^{***}	-1.386	-1.096
22	30	Club_22_30	-0.496	-1.128	1.065
22	31	Club_22_31	-1.106^{***}	-1.175	-0.938
22	34	Club_22_34	-0.037	-0.895	0.606
22	35	Club_22_35	-0.085	-1.175	0.948
22	36	Club_22_36	-1.030^{***}	-1.179	0.044
22	37	Club_22_37	-0.883^{***}	-1.175	-0.777
23	24	Club_23_24	-0.876^{***}	-1.177	-0.138
23	25	Club_23_25	-0.713	-1.041	0.711
23	26	Club_23_26	-0.730	-1.122	0.852
23	27	Club_23_27	-0.783^{***}	-0.996	0.005
23	28	Club_23_28	-0.808	-1.334	0.711
23	29	Club_23_29	-0.958^{***}	-1.327	-0.174
23	30	Club_23_30	-0.098	-1.104	1.065
23	31	Club_23_31	-0.760	-1.091	0.874
23	34	Club_23_34	0.181	-0.659	0.644
23	35	Club_23_35	0.154	-0.712	0.948

Continued on next page

Club1	Club2	Label	$\hat{\theta}_{gh}$	bca_lo	bca_hi
23	36	Club_23_36	-0.788^{***}	-1.179	-0.595
23	37	Club_23_37	-0.668^{***}	-0.687	-0.649
24	25	Club_24_25	-1.007^{***}	-1.477	-0.743
24	26	Club_24_26	-1.022^{***}	-1.177	-0.262
24	27	Club_24_27	-1.075^{***}	-1.177	-0.964
24	28	Club_24_28	-1.124^{***}	-1.442	-0.909
24	29	Club_24_29	-1.158^{***}	-1.386	-1.083
24	30	Club_24_30	-0.355	-1.012	1.065
24	31	Club_24_31	-1.076^{***}	-1.177	-0.956
24	34	Club_24_34	0.071	-0.776	0.614
24	35	Club_24_35	0.031	-0.906	0.948
24	36	Club_24_36	-1.001^{***}	-1.178	0.065
24	37	Club_24_37	-0.844^{***}	-1.177	-0.671
25	26	Club_25_26	-0.840	-1.228	1.011
25	27	Club_25_27	-0.906^{***}	-1.714	-0.799
25	28	Club_25_28	-0.950^{***}	-1.060	-0.800
25	29	Club_25_29	-1.065^{***}	-1.571	-0.921
25	30	Club_25_30	-0.005	-0.838	1.065
25	31	Club_25_31	-0.889^{*}	-1.042	1.044
25	34	Club_25_34	0.263	-0.057	0.621
25	35	Club_25_35	0.242	-0.792	0.948
25	36	Club_25_36	-0.875^{*}	-1.714	0.264
25	37	Club_25_37	-0.720	-1.714	0.106
26	27	Club_26_27	-0.924^{***}	-1.122	-0.026
26	28	Club_26_28	-0.969^{*}	-1.334	0.852
26	29	Club_26_29	-1.074^{***}	-1.386	-0.495
26	30	Club_26_30	-0.041	-1.086	1.065
26	31	Club_26_31	-0.909^{**}	-1.135	0.249
26	34	Club_26_34	0.246	-0.718	0.750

Continued on next page

Club1	Club2	Label	$\hat{\theta}_{gh}$	bca_lo	bca_hi
26	35	Club_26_35	0.222	-1.070	1.011
26	36	Club_26_36	-0.888^{***}	-1.179	-0.039
26	37	Club_26_37	-0.732^{***}	-1.122	-0.183
27	28	Club_27_28	-1.035^{***}	-1.442	-0.798
27	29	Club_27_29	-1.111^{***}	-1.386	-1.016
27	30	Club_27_30	-0.136	-1.070	1.065
27	31	Club_27_31	-0.978^{***}	-1.135	-0.858
27	34	Club_27_34	0.200	-0.704	0.615
27	35	Club_27_35	0.171	-0.862	0.948
27	36	Club_27_36	-0.932^{***}	-1.179	0.170
27	37	Club_27_37	-0.772^{***}	-0.996	-0.701
28	29	Club_28_29	-1.147^{***}	-1.442	-1.017
28	30	Club_28_30	-0.108	-1.099	1.065
28	31	Club_28_31	-1.033^{**}	-1.290	0.329
28	34	Club_28_34	0.226	-0.716	0.621
28	35	Club_28_35	0.199	-1.015	0.948
28	36	Club_28_36	-0.962^{*}	-1.442	0.628
28	37	Club_28_37	-0.790^{**}	-1.442	-0.127
29	30	Club_29_30	-0.627	-1.144	1.065
29	31	Club_29_31	-1.114^{***}	-1.277	-1.039
29	34	Club_29_34	-0.167	-0.929	0.362
29	35	Club_29_35	-0.220	-1.135	0.627
29	36	Club_29_36	-1.047^{***}	-1.327	0.262
29	37	Club_29_37	-0.918^{***}	-1.386	-0.745
30	31	Club_30_31	-0.017	-1.000	1.065
30	34	Club_30_34	0.702^{***}	0.659	1.065
30	35	Club_30_35	0.736^{*}	-0.481	1.065
30	36	Club_30_36	-0.356	-1.359	1.065
30	37	Club_30_37	-0.274	-0.917	1.065

Continued on next page

Club1	Club2	Label	$\hat{\theta}_{gh}$	bca_lo	bca_hi
31	34	Club_31_34	0.268	-0.308	0.741
31	35	Club_31_35	0.246	-0.890	1.044
31	36	Club_31_36	-0.923^{**}	-1.150	0.382
31	37	Club_31_37	-0.754^{***}	-1.135	-0.048
34	35	Club_34_35	0.629^{***}	0.263	0.798
34	36	Club_34_36	0.019	-0.960	0.614
34	37	Club_34_37	0.031	-0.631	0.614
35	36	Club_35_36	-0.021	-1.179	0.734
35	37	Club_35_37	-0.003	-0.688	0.948
36	37	Club_36_37	-0.778^{***}	-0.977	-0.660

Table B.2: Results by club pair, using the selected 5,720 SNPs, with point estimate ($\hat{\theta}_{gh}$) and Bias Corrected and Accelerated Bootstrap CI. Significance stars: $^{*}p < 0.1$, $^{**}p < 0.05$, $^{***}p < 0.01$ (two-sided; p-values inferred from the 95% interval assuming normality).

Club1	Club2	Label	$\hat{\theta}_{gh}$	bca_lo	bca_hi
1	2	Club_1_2	-1.608^{***}	-1.728	-1.180
1	3	Club_1_3	-1.680^{***}	-1.778	-1.605
1	4	Club_1_4	-1.470^{***}	-1.744	-1.376
1	5	Club_1_5	-1.519^{***}	-1.727	-1.173
1	6	Club_1_6	-1.349^{***}	-1.541	-1.017
1	7	Club_1_7	-1.444^{***}	-1.725	-1.299
1	8	Club_1_8	-1.489^{***}	-1.741	-1.363
1	9	Club_1_9	-1.497^{***}	-1.726	-1.450
1	10	Club_1_10	-1.456^{***}	-1.737	-1.433
1	11	Club_1_11	-1.266^{***}	-1.731	-0.952
1	12	Club_1_12	-1.292^{***}	-1.729	-0.779
1	13	Club_1_13	0.360^{**}	-0.035	0.522
1	14	Club_1_14	-1.187^{***}	-1.725	-1.019

Continued on next page

Club1	Club2	Label	$\hat{\theta}_{gh}$	bca_lo	bca_hi
1	15	Club_1_15	0.253	-1.737	0.412
1	16	Club_1_16	0.283	-1.727	0.480
1	17	Club_1_17	-0.312	-1.744	0.232
1	18	Club_1_18	-0.027	-1.739	0.296
1	19	Club_1_19	-1.221^{***}	-1.453	-1.115
1	20	Club_1_20	-0.485^{*}	-0.807	0.323
1	21	Club_1_21	-1.372^{***}	-1.735	-1.234
1	22	Club_1_22	-1.329^{***}	-1.628	-1.079
1	23	Club_1_23	-1.466^{***}	-1.744	-1.349
1	24	Club_1_24	-1.151^{***}	-1.727	-0.230
1	25	Club_1_25	0.154	-1.009	0.518
1	26	Club_1_26	0.227	-1.721	0.237
1	27	Club_1_27	0.348	-1.732	0.532
1	28	Club_1_28	-0.009	-1.743	0.442
1	29	Club_1_29	-0.265	-1.280	0.496
1	30	Club_1_30	0.155	-1.445	0.343
1	31	Club_1_31	-1.457^{***}	-1.719	-1.334
1	32	Club_1_32	-1.465^{***}	-1.739	-1.288
1	33	Club_1_33	-1.402^{***}	-1.595	-1.134
1	34	Club_1_34	-1.471^{***}	-1.721	-1.162
1	35	Club_1_35	-1.406^{***}	-1.580	-0.938
1	36	Club_1_36	-1.695^{***}	-1.773	-1.216
1	37	Club_1_37	-1.679^{***}	-1.734	-1.169
1	38	Club_1_38	-1.623^{***}	-1.812	-1.099
1	39	Club_1_39	-1.432^{***}	-1.731	-1.119
1	40	Club_1_40	-1.510^{***}	-1.741	-1.323
2	3	Club_2_3	-1.607^{***}	-1.769	-1.343
2	4	Club_2_4	-1.384^{***}	-1.555	-0.406
2	5	Club_2_5	-1.428^{***}	-1.598	-0.803

Continued on next page

Club1	Club2	Label	$\hat{\theta}_{gh}$	bca_lo	bca_hi
2	6	Club_2_6	-1.273^{***}	-1.463	-0.823
2	7	Club_2_7	-1.355^{***}	-1.517	-0.820
2	8	Club_2_8	-1.404^{***}	-1.542	-1.041
2	9	Club_2_9	-1.422^{***}	-1.541	-1.034
2	10	Club_2_10	-1.355^{***}	-1.704	-1.052
2	11	Club_2_11	-1.177^{***}	-1.742	-0.597
2	12	Club_2_12	-1.202^{**}	-1.716	0.601
2	13	Club_2_13	0.394^{***}	0.154	0.615
2	14	Club_2_14	-1.105^{***}	-1.457	-0.698
2	15	Club_2_15	0.300	-1.811	0.453
2	16	Club_2_16	0.326	-1.617	0.620
2	17	Club_2_17	-0.215	-1.766	0.262
2	18	Club_2_18	0.049	-1.777	0.336
2	19	Club_2_19	-1.146^{***}	-1.744	-0.297
2	20	Club_2_20	-0.376	-0.636	0.694
2	21	Club_2_21	-1.281^{***}	-1.771	-1.020
2	22	Club_2_22	-1.237^{***}	-1.454	-0.622
2	23	Club_2_23	-1.364^{***}	-1.732	-0.982
2	24	Club_2_24	-1.036^{**}	-1.733	0.315
2	25	Club_2_25	0.210	-0.838	0.623
2	26	Club_2_26	0.277	-1.759	0.344
2	27	Club_2_27	0.383	-1.747	0.542
2	28	Club_2_28	0.065	-1.784	0.440
2	29	Club_2_29	-0.153	-1.208	0.923
2	30	Club_2_30	0.213	-0.710	0.404
2	31	Club_2_31	-1.374^{***}	-1.525	-1.030
2	32	Club_2_32	-1.373^{***}	-1.579	-0.841
2	33	Club_2_33	-1.318^{***}	-1.482	-0.847
2	34	Club_2_34	-1.386^{***}	-1.543	-0.818

Continued on next page

Club1	Club2	Label	$\hat{\theta}_{gh}$	bca_lo	bca_hi
2	35	Club_2_35	-1.329^{***}	-1.507	-0.311
2	36	Club_2_36	-1.640^{***}	-1.769	-1.190
2	37	Club_2_37	-1.609^{***}	-1.732	-1.162
2	38	Club_2_38	-1.556^{***}	-1.803	-0.493
2	39	Club_2_39	-1.352^{***}	-1.588	-0.351
2	40	Club_2_40	-1.421^{***}	-1.604	-0.705
3	4	Club_3_4	-1.352^{***}	-1.775	-1.248
3	5	Club_3_5	-1.427^{***}	-1.736	-1.171
3	6	Club_3_6	-1.195^{***}	-1.433	-0.979
3	7	Club_3_7	-1.299^{***}	-1.644	-1.065
3	8	Club_3_8	-1.386^{***}	-1.563	-1.300
3	9	Club_3_9	-1.418^{***}	-1.524	-1.374
3	10	Club_3_10	-1.283^{***}	-1.577	-1.255
3	11	Club_3_11	-1.029^{***}	-1.719	-0.610
3	12	Club_3_12	-1.062^{**}	-1.635	0.137
3	13	Club_3_13	0.515^{***}	0.440	0.664
3	14	Club_3_14	-0.953^{***}	-1.601	-0.781
3	15	Club_3_15	0.470^{***}	0.260	0.655
3	16	Club_3_16	0.484^{***}	0.345	1.028
3	17	Club_3_17	0.161	-1.652	0.625
3	18	Club_3_18	0.336	-1.470	0.665
3	19	Club_3_19	-1.024^{***}	-1.556	-0.881
3	20	Club_3_20	0.040	0.032	0.894
3	21	Club_3_21	-1.179^{***}	-1.877	-1.032
3	22	Club_3_22	-1.107^{***}	-1.579	-0.845
3	23	Club_3_23	-1.299^{***}	-1.661	-1.177
3	24	Club_3_24	-0.723	-1.528	1.036
3	25	Club_3_25	0.420^{*}	0.329	1.202
3	26	Club_3_26	0.462	-1.463	0.615

Continued on next page

Club1	Club2	Label	$\hat{\theta}_{gh}$	bca_lo	bca_hi
3	27	Club_3_27	0.510^{***}	0.380	1.027
3	28	Club_3_28	0.344	-1.703	0.624
3	29	Club_3_29	0.308	0.068	0.954
3	30	Club_3_30	0.428^{***}	0.300	0.774
3	31	Club_3_31	-1.338^{***}	-1.703	-1.159
3	32	Club_3_32	-1.327^{***}	-1.644	-1.073
3	33	Club_3_33	-1.248^{***}	-1.751	-1.051
3	34	Club_3_34	-1.355^{***}	-1.654	-1.116
3	35	Club_3_35	-1.273^{***}	-1.618	-1.062
3	36	Club_3_36	-1.748^{***}	-1.836	-1.711
3	37	Club_3_37	-1.739^{***}	-1.824	-1.740
3	38	Club_3_38	-1.633^{***}	-1.920	-1.314
3	39	Club_3_39	-1.305^{***}	-1.799	-1.091
3	40	Club_3_40	-1.414^{***}	-1.751	-1.252
4	5	Club_4_5	-1.028^{***}	-1.182	0.103
4	6	Club_4_6	-0.966^{***}	-1.048	0.210
4	7	Club_4_7	-0.956^{***}	-1.085	0.255
4	8	Club_4_8	-1.048^{***}	-1.232	-1.018
4	9	Club_4_9	-1.131^{***}	-1.242	-1.095
4	10	Club_4_10	-0.858^{***}	-1.075	-0.793
4	11	Club_4_11	-0.775	-1.019	1.088
4	12	Club_4_12	-0.794	-1.018	1.086
4	13	Club_4_13	0.533^{***}	0.489	0.673
4	14	Club_4_14	-0.750^{***}	-0.821	0.154
4	15	Club_4_15	0.498	-1.037	0.665
4	16	Club_4_16	0.510^{***}	0.387	1.077
4	17	Club_4_17	0.257	-1.186	0.499
4	18	Club_4_18	0.394	-1.027	0.675
4	19	Club_4_19	-0.835^{***}	-1.018	0.206

Continued on next page

Club1	Club2	Label	$\hat{\theta}_{gh}$	bca_lo	bca_hi
4	20	Club_4_20	0.167	0.185	1.080
4	21	Club_4_21	-0.872^{***}	-1.235	-0.753
4	22	Club_4_22	-0.812^{**}	-0.889	0.421
4	23	Club_4_23	-0.859^{***}	-1.043	-0.690
4	24	Club_4_24	-0.413	-1.017	1.088
4	25	Club_4_25	0.457^{**}	0.352	1.212
4	26	Club_4_26	0.493	-1.059	0.539
4	27	Club_4_27	0.530^{***}	0.408	1.082
4	28	Club_4_28	0.399	-1.112	0.650
4	29	Club_4_29	0.414^{*}	0.151	1.000
4	30	Club_4_30	0.465^{***}	0.358	0.699
4	31	Club_4_31	-1.029^{***}	-1.192	-0.195
4	32	Club_4_32	-0.956^{***}	-1.115	0.156
4	33	Club_4_33	-0.960^{***}	-1.066	0.207
4	34	Club_4_34	-1.022^{*}	-1.062	1.070
4	35	Club_4_35	-1.017^{***}	-1.162	0.078
4	36	Club_4_36	-1.481^{***}	-1.817	-1.380
4	37	Club_4_37	-1.373^{***}	-1.731	-1.001
4	38	Club_4_38	-1.328^{***}	-1.630	-0.463
4	39	Club_4_39	-1.022^{***}	-1.348	-0.955
4	40	Club_4_40	-1.029^{***}	-1.173	-0.420
5	6	Club_5_6	-0.965^{***}	-1.059	-0.860
5	7	Club_5_7	-0.954^{***}	-1.189	-0.884
5	8	Club_5_8	-1.062^{***}	-1.222	-1.016
5	9	Club_5_9	-1.155^{***}	-1.286	-1.032
5	10	Club_5_10	-0.831^{***}	-1.082	-0.774
5	11	Club_5_11	-0.747^{***}	-1.088	-0.594
5	12	Club_5_12	-0.768^{***}	-1.068	-0.092
5	13	Club_5_13	0.556^{***}	0.479	0.625

Continued on next page

Club1	Club2	Label	$\hat{\theta}_{gh}$	bca_lo	bca_hi
5	14	Club_5_14	-0.725^{***}	-1.008	-0.616
5	15	Club_5_15	0.531	-1.494	0.577
5	16	Club_5_16	0.540	-1.058	0.624
5	17	Club_5_17	0.346	-1.416	0.531
5	18	Club_5_18	0.455	-1.424	0.556
5	19	Club_5_19	-0.821^{**}	-1.034	0.246
5	20	Club_5_20	0.274^{**}	0.194	0.700
5	21	Club_5_21	-0.855^{***}	-1.420	-0.750
5	22	Club_5_22	-0.786^{***}	-0.875	-0.568
5	23	Club_5_23	-0.831^{***}	-1.109	-0.744
5	24	Club_5_24	-0.303	-1.069	0.316
5	25	Club_5_25	0.499^{***}	0.386	0.624
5	26	Club_5_26	0.530	-1.408	0.556
5	27	Club_5_27	0.554	-1.078	0.619
5	28	Club_5_28	0.458	-1.416	0.580
5	29	Club_5_29	0.533	-0.803	0.926
5	30	Club_5_30	0.509^{***}	0.224	0.625
5	31	Club_5_31	-1.038^{***}	-1.188	-0.872
5	32	Club_5_32	-0.953^{***}	-1.224	-0.875
5	33	Club_5_33	-0.959^{***}	-1.070	-0.822
5	34	Club_5_34	-1.032^{***}	-1.073	-0.908
5	35	Club_5_35	-1.024^{***}	-1.202	0.239
5	36	Club_5_36	-1.545^{***}	-1.813	-1.066
5	37	Club_5_37	-1.446^{***}	-1.648	-1.007
5	38	Club_5_38	-1.381^{***}	-1.693	-0.978
5	39	Club_5_39	-1.030^{***}	-1.388	-0.267
5	40	Club_5_40	-1.041^{***}	-1.163	-0.983
6	7	Club_6_7	-0.920^{***}	-1.023	-0.833
6	8	Club_6_8	-0.986^{***}	-1.067	-0.848

Continued on next page

Club1	Club2	Label	$\hat{\theta}_{gh}$	bca_lo	bca_hi
6	9	Club_6_9	-1.055^{***}	-1.197	-0.871
6	10	Club_6_10	-0.849^{***}	-1.065	-0.723
6	11	Club_6_11	-0.789^{***}	-0.981	-0.640
6	12	Club_6_12	-0.804^{***}	-0.994	-0.316
6	13	Club_6_13	0.481^{***}	0.362	0.560
6	14	Club_6_14	-0.768^{***}	-0.858	-0.680
6	15	Club_6_15	0.424	-1.297	0.512
6	16	Club_6_16	0.441	-0.967	0.555
6	17	Club_6_17	0.091	-1.291	0.392
6	18	Club_6_18	0.268	-1.243	0.435
6	19	Club_6_19	-0.834^{***}	-0.963	0.116
6	20	Club_6_20	-0.018	-0.207	0.276
6	21	Club_6_21	-0.861^{***}	-1.291	-0.746
6	22	Club_6_22	-0.817^{***}	-0.903	-0.588
6	23	Club_6_23	-0.850^{***}	-1.031	-0.681
6	24	Club_6_24	-0.541^{**}	-1.057	-0.059
6	25	Club_6_25	0.366^{***}	0.154	0.614
6	26	Club_6_26	0.413	-1.216	0.433
6	27	Club_6_27	0.475	-1.107	0.563
6	28	Club_6_28	0.277	-1.291	0.507
6	29	Club_6_29	0.199	-0.856	0.581
6	30	Club_6_30	0.372^{***}	0.035	0.481
6	31	Club_6_31	-0.975^{***}	-1.055	-0.812
6	32	Club_6_32	-0.918^{***}	-1.034	-0.833
6	33	Club_6_33	-0.927^{***}	-0.980	-0.839
6	34	Club_6_34	-0.968^{***}	-1.051	-0.839
6	35	Club_6_35	-0.973^{***}	-1.090	0.044
6	36	Club_6_36	-1.335^{***}	-1.544	-0.929
6	37	Club_6_37	-1.218^{***}	-1.386	-0.872

Continued on next page

Club1	Club2	Label	$\hat{\theta}_{gh}$	bca_lo	bca_hi
6	38	Club_6_38	-1.201^{***}	-1.455	-0.344
6	39	Club_6_39	-0.974^{***}	-1.072	0.375
6	40	Club_6_40	-0.967^{***}	-1.052	-0.072
7	8	Club_7_8	-0.986^{***}	-1.176	-0.928
7	9	Club_7_9	-1.082^{***}	-1.249	-0.962
7	10	Club_7_10	-0.767^{***}	-1.054	-0.729
7	11	Club_7_11	-0.716^{***}	-0.889	-0.627
7	12	Club_7_12	-0.733^{***}	-0.888	0.062
7	13	Club_7_13	0.545^{***}	0.506	0.616
7	14	Club_7_14	-0.701^{***}	-0.799	-0.653
7	15	Club_7_15	0.516	-1.139	0.564
7	16	Club_7_16	0.526^{***}	0.318	0.591
7	17	Club_7_17	0.307	-1.287	0.496
7	18	Club_7_18	0.427	-0.957	0.530
7	19	Club_7_19	-0.792^{***}	-0.889	0.286
7	20	Club_7_20	0.230^{***}	0.201	0.385
7	21	Club_7_21	-0.806^{***}	-0.959	-0.719
7	22	Club_7_22	-0.745^{***}	-0.798	-0.568
7	23	Club_7_23	-0.765^{***}	-1.270	-0.706
7	24	Club_7_24	-0.317	-0.888	0.315
7	25	Club_7_25	0.480^{***}	0.444	0.621
7	26	Club_7_26	0.513	-0.930	0.536
7	27	Club_7_27	0.542	-0.886	0.592
7	28	Club_7_28	0.431	-1.266	0.550
7	29	Club_7_29	0.476^{**}	0.190	0.920
7	30	Club_7_30	0.489^{***}	0.349	0.568
7	31	Club_7_31	-0.971^{***}	-1.127	-0.827
7	32	Club_7_32	-0.882^{***}	-1.054	-0.825
7	33	Club_7_33	-0.903^{***}	-1.020	-0.835

Continued on next page

Club1	Club2	Label	$\hat{\theta}_{gh}$	bca_lo	bca_hi
7	34	Club_7_34	-0.960^{***}	-1.100	-0.880
7	35	Club_7_35	-0.969^{***}	-1.179	-0.800
7	36	Club_7_36	-1.450^{***}	-1.638	-1.064
7	37	Club_7_37	-1.325^{***}	-1.497	-0.880
7	38	Club_7_38	-1.285^{***}	-1.561	-0.884
7	39	Club_7_39	-0.969^{***}	-1.307	-0.821
7	40	Club_7_40	-0.957^{***}	-1.100	-0.868
8	9	Club_8_9	-1.156^{***}	-1.217	-1.087
8	10	Club_8_10	-0.894^{***}	-1.076	-0.861
8	11	Club_8_11	-0.797^{***}	-1.078	-0.656
8	12	Club_8_12	-0.818^{***}	-1.082	-0.323
8	13	Club_8_13	0.532^{***}	0.482	0.615
8	14	Club_8_14	-0.768^{***}	-1.053	-0.692
8	15	Club_8_15	0.496	-1.152	0.556
8	16	Club_8_16	0.507^{***}	0.296	0.617
8	17	Club_8_17	0.249	-1.151	0.468
8	18	Club_8_18	0.389	-1.149	0.522
8	19	Club_8_19	-0.852^{***}	-1.107	0.069
8	20	Club_8_20	0.156^{**}	0.125	0.405
8	21	Club_8_21	-0.898^{***}	-1.171	-0.818
8	22	Club_8_22	-0.837^{***}	-0.934	-0.569
8	23	Club_8_23	-0.896^{***}	-1.150	-0.795
8	24	Club_8_24	-0.439	-1.077	0.316
8	25	Club_8_25	0.454^{***}	0.336	0.612
8	26	Club_8_26	0.491	-1.098	0.528
8	27	Club_8_27	0.528	-1.061	0.584
8	28	Club_8_28	0.394	-1.150	0.547
8	29	Club_8_29	0.405^{*}	0.003	0.922
8	30	Club_8_30	0.462^{***}	0.293	0.550

Continued on next page

Club1	Club2	Label	$\hat{\theta}_{gh}$	bca_lo	bca_hi
8	31	Club_8_31	-1.055^{***}	-1.187	-0.945
8	32	Club_8_32	-0.987^{***}	-1.188	-0.921
8	33	Club_8_33	-0.985^{***}	-1.082	-0.873
8	34	Club_8_34	-1.051^{***}	-1.104	-0.835
8	35	Club_8_35	-1.040^{***}	-1.194	-0.280
8	36	Club_8_36	-1.505^{***}	-1.677	-1.149
8	37	Club_8_37	-1.405^{***}	-1.556	-1.047
8	38	Club_8_38	-1.355^{***}	-1.592	-1.009
8	39	Club_8_39	-1.047^{***}	-1.389	-0.992
8	40	Club_8_40	-1.062^{***}	-1.271	-1.031
9	10	Club_9_10	-1.027^{***}	-1.209	-1.010
9	11	Club_9_11	-0.901^{***}	-1.234	-0.723
9	12	Club_9_12	-0.923^{***}	-1.208	-0.617
9	13	Club_9_13	0.493^{***}	0.438	0.551
9	14	Club_9_14	-0.858^{***}	-1.208	-0.751
9	15	Club_9_15	0.440	-1.229	0.509
9	16	Club_9_16	0.456^{***}	0.050	0.555
9	17	Club_9_17	0.107	-1.238	0.395
9	18	Club_9_18	0.289	-1.227	0.450
9	19	Club_9_19	-0.926^{***}	-1.031	-0.220
9	20	Club_9_20	-0.011	-0.029	0.279
9	21	Club_9_21	-1.002^{***}	-1.261	-0.871
9	22	Club_9_22	-0.948^{***}	-1.205	-0.807
9	23	Club_9_23	-1.033^{***}	-1.216	-0.943
9	24	Club_9_24	-0.633^{**}	-1.207	-0.093
9	25	Club_9_25	0.384^{***}	0.291	0.534
9	26	Club_9_26	0.430	-1.226	0.456
9	27	Club_9_27	0.487	-1.084	0.558
9	28	Club_9_28	0.298	-1.225	0.498

Continued on next page

Club1	Club2	Label	$\hat{\theta}_{gh}$	bca_lo	bca_hi
9	29	Club_9_29	0.228	-0.831	0.566
9	30	Club_9_30	0.391^{***}	0.146	0.478
9	31	Club_9_31	-1.132^{***}	-1.234	-1.033
9	32	Club_9_32	-1.090^{***}	-1.243	-0.969
9	33	Club_9_33	-1.069^{***}	-1.205	-0.899
9	34	Club_9_34	-1.134^{***}	-1.213	-1.017
9	35	Club_9_35	-1.108^{***}	-1.239	-0.872
9	36	Club_9_36	-1.513^{***}	-1.584	-1.460
9	37	Club_9_37	-1.432^{***}	-1.566	-1.289
9	38	Club_9_38	-1.385^{***}	-1.610	-1.099
9	39	Club_9_39	-1.120^{***}	-1.428	-1.027
9	40	Club_9_40	-1.152^{***}	-1.229	-1.036
10	11	Club_10_11	-0.592^{***}	-0.746	-0.568
10	12	Club_10_12	-0.606^{***}	-0.739	-0.584
10	13	Club_10_13	0.582^{***}	0.577	0.614
10	14	Club_10_14	-0.603^{***}	-0.679	-0.585
10	15	Club_10_15	0.570^{***}	0.531	0.619
10	16	Club_10_16	0.575^{***}	0.553	0.625
10	17	Club_10_17	0.465	-0.562	0.557
10	18	Club_10_18	0.530^{***}	0.394	0.628
10	19	Club_10_19	-0.716^{***}	-0.757	-0.739
10	20	Club_10_20	0.426	0.447	0.447
10	21	Club_10_21	-0.678^{***}	-0.743	-0.694
10	22	Club_10_22	-0.607^{***}	-0.686	-0.565
10	23	Club_10_23	-0.550^{***}	-0.562	-0.550
10	24	Club_10_24	-0.031	-0.481	0.160
10	25	Club_10_25	0.549^{***}	0.553	0.623
10	26	Club_10_26	0.572^{***}	0.521	0.617
10	27	Club_10_27	0.581^{***}	0.549	0.622

Continued on next page

Club1	Club2	Label	$\hat{\theta}_{gh}$	bca_lo	bca_hi
10	28	Club_10_28	0.531^{*}	-0.562	0.587
10	29	Club_10_29	0.682^{***}	0.665	0.918
10	30	Club_10_30	0.560^{***}	0.536	0.628
10	31	Club_10_31	-0.885^{***}	-1.190	-0.781
10	32	Club_10_32	-0.747^{***}	-1.254	-0.685
10	33	Club_10_33	-0.807^{***}	-0.959	-0.607
10	34	Club_10_34	-0.864^{***}	-1.153	-0.846
10	35	Club_10_35	-0.899^{***}	-1.276	-0.786
10	36	Club_10_36	-1.466^{***}	-1.826	-1.408
10	37	Club_10_37	-1.318^{***}	-1.740	-1.175
10	38	Club_10_38	-1.271^{***}	-1.567	-0.887
10	39	Club_10_39	-0.891^{***}	-1.290	-0.816
10	40	Club_10_40	-0.841^{***}	-1.047	-0.759
11	12	Club_11_12	-0.614^{***}	-0.665	-0.561
11	13	Club_11_13	0.530^{***}	0.403	0.625
11	14	Club_11_14	-0.610^{***}	-0.638	-0.551
11	15	Club_11_15	0.494	-0.664	0.620
11	16	Club_11_16	0.506	-0.595	0.625
11	17	Club_11_17	0.267	-0.785	0.625
11	18	Club_11_18	0.393	-0.767	0.627
11	19	Club_11_19	-0.695^{***}	-0.762	0.257
11	20	Club_11_20	0.190	0.077	0.699
11	21	Club_11_21	-0.661^{***}	-0.825	-0.614
11	22	Club_11_22	-0.615^{***}	-0.652	-0.568
11	23	Club_11_23	-0.587^{***}	-0.746	-0.544
11	24	Club_11_24	-0.265	-0.612	0.316
11	25	Club_11_25	0.454^{***}	0.255	0.624
11	26	Club_11_26	0.489	-0.787	0.550
11	27	Club_11_27	0.526^{*}	-0.620	0.626

Continued on next page

Club1	Club2	Label	$\hat{\theta}_{gh}$	bca_lo	bca_hi
11	28	Club_11_28	0.398	-0.785	0.623
11	29	Club_11_29	0.410	-0.656	0.925
11	30	Club_11_30	0.462^{***}	0.234	0.626
11	31	Club_11_31	-0.797^{***}	-1.039	-0.604
11	32	Club_11_32	-0.700^{***}	-0.882	-0.574
11	33	Club_11_33	-0.749^{***}	-0.915	-0.581
11	34	Club_11_34	-0.779^{***}	-1.141	-0.613
11	35	Club_11_35	-0.819^{***}	-1.258	-0.580
11	36	Club_11_36	-1.233^{***}	-1.823	-0.905
11	37	Club_11_37	-1.066^{***}	-1.730	-0.596
11	38	Club_11_38	-1.065^{***}	-1.887	-0.697
11	39	Club_11_39	-0.808^{***}	-1.111	-0.314
11	40	Club_11_40	-0.756^{***}	-1.048	-0.567
12	13	Club_12_13	0.535^{*}	-0.609	0.616
12	14	Club_12_14	-0.619^{***}	-0.648	-0.549
12	15	Club_12_15	0.501	-0.707	0.619
12	16	Club_12_16	0.512	-0.708	0.625
12	17	Club_12_17	0.281	-0.714	0.624
12	18	Club_12_18	0.403	-0.716	0.626
12	19	Club_12_19	-0.705^{**}	-0.757	0.531
12	20	Club_12_20	0.204	-0.080	0.700
12	21	Club_12_21	-0.674^{***}	-0.823	-0.617
12	22	Club_12_22	-0.626^{***}	-0.662	0.096
12	23	Club_12_23	-0.601^{***}	-0.729	-0.539
12	24	Club_12_24	-0.261	-0.636	0.601
12	25	Club_12_25	0.462	-0.611	0.625
12	26	Club_12_26	0.496	-0.675	0.567
12	27	Club_12_27	0.531	-0.700	0.621
12	28	Club_12_28	0.408	-0.739	0.623

Continued on next page

Club1	Club2	Label	$\hat{\theta}_{gh}$	bca_lo	bca_hi
12	29	Club_12_29	0.429	-0.738	0.925
12	30	Club_12_30	0.470	-0.663	0.626
12	31	Club_12_31	-0.817^{***}	-1.037	-0.228
12	32	Club_12_32	-0.718^{***}	-0.868	-0.204
12	33	Club_12_33	-0.765^{***}	-0.862	-0.251
12	34	Club_12_34	-0.798^{***}	-1.066	-0.109
12	35	Club_12_35	-0.837^{*}	-1.260	0.645
12	36	Club_12_36	-1.263^{***}	-1.820	-0.643
12	37	Club_12_37	-1.099^{***}	-1.729	-0.480
12	38	Club_12_38	-1.093^{**}	-1.834	0.049
12	39	Club_12_39	-0.826	-1.036	1.218
12	40	Club_12_40	-0.776	-1.044	1.068
13	14	Club_13_14	0.499^{***}	0.434	0.620
13	15	Club_13_15	0.616^{***}	0.611	0.622
13	16	Club_13_16	0.616^{***}	0.612	0.621
13	17	Club_13_17	0.616^{***}	0.456	0.618
13	18	Club_13_18	0.618^{***}	0.612	0.625
13	19	Club_13_19	0.471	-0.752	0.652
13	20	Club_13_20	0.617^{***}	0.540	0.658
13	21	Club_13_21	0.542^{***}	0.481	0.625
13	22	Club_13_22	0.545^{***}	0.477	0.615
13	23	Club_13_23	0.585^{***}	0.573	0.625
13	24	Club_13_24	0.602^{***}	0.548	0.615
13	25	Club_13_25	0.614^{***}	0.303	0.624
13	26	Club_13_26	0.619^{***}	0.614	0.625
13	27	Club_13_27	0.615^{***}	0.608	0.617
13	28	Club_13_28	0.617^{***}	0.610	0.624
13	29	Club_13_29	0.654^{***}	0.425	0.920
13	30	Club_13_30	0.618^{***}	0.536	0.619

Continued on next page

Club1	Club2	Label	$\hat{\theta}_{gh}$	bca_lo	bca_hi
13	31	Club_13_31	0.521***	0.483	0.616
13	32	Club_13_32	0.556***	0.522	0.615
13	33	Club_13_33	0.520***	0.465	0.625
13	34	Club_13_34	0.533***	0.417	0.615
13	35	Club_13_35	0.492***	0.287	0.614
13	36	Club_13_36	0.418***	0.274	0.624
13	37	Club_13_37	0.499***	0.402	0.625
13	38	Club_13_38	0.474***	0.411	0.657
13	39	Club_13_39	0.508***	0.380	0.658
13	40	Club_13_40	0.552***	0.464	0.649
14	15	Club_14_15	0.451	-0.664	0.533
14	16	Club_14_16	0.465***	0.257	0.624
14	17	Club_14_17	0.174	-0.687	0.425
14	18	Club_14_18	0.320	-0.685	0.477
14	19	Club_14_19	−0.688***	-0.755	0.135
14	20	Club_14_20	0.086	0.035	0.261
14	21	Club_14_21	−0.657***	-0.743	-0.630
14	22	Club_14_22	−0.620***	-0.640	-0.556
14	23	Club_14_23	−0.599***	-0.671	-0.574
14	24	Club_14_24	−0.340**	-0.620	-0.029
14	25	Club_14_25	0.401***	0.322	0.612
14	26	Club_14_26	0.442	-0.652	0.487
14	27	Club_14_27	0.494	-0.614	0.620
14	28	Club_14_28	0.327	-0.687	0.505
14	29	Club_14_29	0.288	-0.139	0.923
14	30	Club_14_30	0.407***	0.255	0.626
14	31	Club_14_31	−0.770***	-0.884	-0.619
14	32	Club_14_32	−0.688***	-0.749	-0.608
14	33	Club_14_33	−0.731***	-0.804	-0.553

Continued on next page

Club1	Club2	Label	$\hat{\theta}_{gh}$	bca_lo	bca_hi
14	34	Club_14_34	-0.753^{***}	-1.146	-0.693
14	35	Club_14_35	-0.791^{***}	-1.026	-0.667
14	36	Club_14_36	-1.144^{***}	-1.815	-0.889
14	37	Club_14_37	-0.986^{***}	-1.212	-0.614
14	38	Club_14_38	-0.993^{***}	-1.252	-0.623
14	39	Club_14_39	-0.780^{***}	-1.032	-0.552
14	40	Club_14_40	-0.732^{***}	-0.853	-0.609
15	16	Club_15_16	0.619^{***}	0.614	0.626
15	17	Club_15_17	0.620^{***}	0.504	0.630
15	18	Club_15_18	0.622^{***}	0.617	0.632
15	19	Club_15_19	0.411	-0.756	0.542
15	20	Club_15_20	0.622^{***}	0.553	0.698
15	21	Club_15_21	0.511^{***}	0.363	0.631
15	22	Club_15_22	0.516	-0.716	0.565
15	23	Club_15_23	0.575^{***}	0.460	0.619
15	24	Club_15_24	0.600^{***}	0.306	0.618
15	25	Club_15_25	0.616^{*}	-0.611	0.632
15	26	Club_15_26	0.622^{***}	0.617	0.632
15	27	Club_15_27	0.617^{***}	0.614	0.619
15	28	Club_15_28	0.621^{***}	0.617	0.632
15	29	Club_15_29	0.674^{***}	0.621	0.926
15	30	Club_15_30	0.621^{***}	0.573	0.630
15	31	Club_15_31	0.480	-1.174	0.553
15	32	Club_15_32	0.531	-0.880	0.631
15	33	Club_15_33	0.479	-1.168	0.555
15	34	Club_15_34	0.497	-1.169	0.547
15	35	Club_15_35	0.439	-1.287	0.510
15	36	Club_15_36	0.332	-1.834	0.433
15	37	Club_15_37	0.448	-1.724	0.620

Continued on next page

Club1	Club2	Label	$\hat{\theta}_{gh}$	bca_lo	bca_hi
15	38	Club_15_38	0.411	-1.889	0.525
15	39	Club_15_39	0.461	-1.567	0.618
15	40	Club_15_40	0.525	-1.061	0.620
16	17	Club_16_17	0.621***	0.487	0.625
16	18	Club_16_18	0.622***	0.616	0.625
16	19	Club_16_19	0.429	-0.757	0.633
16	20	Club_16_20	0.622***	0.527	0.652
16	21	Club_16_21	0.522***	0.390	0.625
16	22	Club_16_22	0.526*	-0.649	0.584
16	23	Club_16_23	0.580***	0.541	0.625
16	24	Club_16_24	0.602***	0.306	0.624
16	25	Club_16_25	0.616*	-0.610	0.625
16	26	Club_16_26	0.622***	0.617	0.629
16	27	Club_16_27	0.617***	0.614	0.619
16	28	Club_16_28	0.621***	0.615	0.624
16	29	Club_16_29	0.670***	0.433	0.926
16	30	Club_16_30	0.622***	0.512	0.625
16	31	Club_16_31	0.493***	0.355	0.625
16	32	Club_16_32	0.540***	0.428	0.625
16	33	Club_16_33	0.492***	0.292	0.624
16	34	Club_16_34	0.508	-1.112	0.588
16	35	Club_16_35	0.455	-1.259	0.565
16	36	Club_16_36	0.357	-1.749	0.616
16	37	Club_16_37	0.463***	0.241	0.625
16	38	Club_16_38	0.430***	0.215	0.622
16	39	Club_16_39	0.476	-1.009	0.635
16	40	Club_16_40	0.534***	0.302	0.625
17	18	Club_17_18	0.628***	0.627	0.633
17	19	Club_17_19	0.083	-0.756	0.415

Continued on next page

Club1	Club2	Label	$\hat{\theta}_{gh}$	bca_lo	bca_hi
17	20	Club_17_20	0.631^{***}	0.513	0.697
17	21	Club_17_21	0.302	-0.823	0.540
17	22	Club_17_22	0.317	-0.778	0.504
17	23	Club_17_23	0.480	-0.657	0.565
17	24	Club_17_24	0.566^{*}	-0.717	0.620
17	25	Club_17_25	0.616^{*}	-0.682	0.628
17	26	Club_17_26	0.626^{***}	0.626	0.640
17	27	Club_17_27	0.617^{*}	-0.717	0.619
17	28	Club_17_28	0.625^{***}	0.624	0.639
17	29	Club_17_29	0.758^{***}	0.682	0.925
17	30	Club_17_30	0.625^{***}	0.404	0.627
17	31	Club_17_31	0.211	-1.228	0.446
17	32	Club_17_32	0.349	-1.224	0.531
17	33	Club_17_33	0.215	-1.224	0.466
17	34	Club_17_34	0.254	-1.156	0.500
17	35	Club_17_35	0.116	-1.287	0.420
17	36	Club_17_36	-0.168	-1.845	0.289
17	37	Club_17_37	0.101	-1.742	0.439
17	38	Club_17_38	0.020	-1.913	0.372
17	39	Club_17_39	0.166	-1.601	0.622
17	40	Club_17_40	0.327	-1.072	0.624
18	19	Club_18_19	0.252	-0.756	0.623
18	20	Club_18_20	0.632^{***}	0.628	0.700
18	21	Club_18_21	0.421	-0.689	0.628
18	22	Club_18_22	0.430	-0.725	0.531
18	23	Club_18_23	0.540^{*}	-0.504	0.628
18	24	Club_18_24	0.591^{***}	0.306	0.627
18	25	Club_18_25	0.619^{*}	-0.613	0.629
18	26	Club_18_26	0.627^{***}	0.628	0.630

Continued on next page

Club1	Club2	Label	$\hat{\theta}_{gh}$	bca_lo	bca_hi
18	27	Club_18_27	0.619^{***}	0.614	0.621
18	28	Club_18_28	0.627^{***}	0.625	0.643
18	29	Club_18_29	0.723^{***}	0.633	0.926
18	30	Club_18_30	0.627^{***}	0.625	0.638
18	31	Club_18_31	0.361	-1.198	0.494
18	32	Club_18_32	0.455	-0.910	0.624
18	33	Club_18_33	0.362	-1.202	0.507
18	34	Club_18_34	0.392	-1.148	0.510
18	35	Club_18_35	0.290	-1.283	0.458
18	36	Club_18_36	0.095	-1.838	0.347
18	37	Club_18_37	0.295	-1.739	0.529
18	38	Club_18_38	0.233	-1.914	0.445
18	39	Club_18_39	0.328	-1.505	0.625
18	40	Club_18_40	0.442	-1.051	0.628
19	20	Club_19_20	-0.018	-0.969	0.818
19	21	Club_19_21	-0.747^{***}	-0.777	-0.727
19	22	Club_19_22	-0.711^{**}	-0.755	0.418
19	23	Club_19_23	-0.714^{***}	-0.795	-0.708
19	24	Club_19_24	-0.464	-0.757	0.655
19	25	Club_19_25	0.352	-0.755	0.925
19	26	Club_19_26	0.399	-0.757	0.403
19	27	Club_19_27	0.464	-0.759	0.627
19	28	Club_19_28	0.262	-0.795	0.629
19	29	Club_19_29	0.180	-0.758	0.811
19	30	Club_19_30	0.357^{*}	-0.137	0.632
19	31	Club_19_31	-0.849^{***}	-1.040	0.186
19	32	Club_19_32	-0.784^{**}	-0.981	0.294
19	33	Club_19_33	-0.810^{**}	-1.005	0.273
19	34	Club_19_34	-0.837^{***}	-1.140	0.089

Continued on next page

Club1	**Club2**	**Label**	$\hat{\theta}_{gh}$	**bca_lo**	**bca_hi**
19	35	Club_19_35	-0.861^{***}	-1.266	-0.012
19	36	Club_19_36	-1.187^{***}	-1.757	-0.556
19	37	Club_19_37	-1.052^{***}	-1.355	-0.013
19	38	Club_19_38	-1.052^{**}	-1.890	-0.047
19	39	Club_19_39	-0.854^{***}	-1.093	0.037
19	40	Club_19_40	-0.826^{**}	-1.062	0.215
20	21	Club_20_21	0.226^{**}	0.308	0.698
20	22	Club_20_22	0.246^{***}	0.197	0.404
20	23	Club_20_23	0.445^{***}	0.483	0.660
20	24	Club_20_24	0.558^{***}	0.059	0.700
20	25	Club_20_25	0.617^{***}	0.395	0.700
20	26	Club_20_26	0.628^{***}	0.627	0.694
20	27	Club_20_27	0.618^{***}	0.512	0.699
20	28	Club_20_28	0.629^{***}	0.623	0.700
20	29	Club_20_29	0.787^{***}	0.452	0.922
20	30	Club_20_30	0.628^{***}	0.495	0.641
20	31	Club_20_31	0.113^{***}	0.135	0.280
20	32	Club_20_32	0.279^{**}	0.255	0.694
20	33	Club_20_33	0.121	0.142	0.627
20	34	Club_20_34	0.163	-0.094	0.698
20	35	Club_20_35	0.006	-0.420	0.700
20	36	Club_20_36	-0.336	-0.612	0.627
20	37	Club_20_37	-0.030	-0.043	0.694
20	38	Club_20_38	-0.119	-0.104	0.287
20	39	Club_20_39	0.062	-0.067	0.737
20	40	Club_20_40	0.251^{**}	0.212	0.692
21	22	Club_21_22	-0.681^{***}	-0.738	-0.620
21	23	Club_21_23	-0.673^{***}	-0.741	-0.649
21	24	Club_21_24	-0.279	-0.634	0.316

Continued on next page

Club1	Club2	Label	$\hat{\theta}_{gh}$	bca_lo	bca_hi
21	25	Club_21_25	0.475^{***}	0.457	0.619
21	26	Club_21_26	0.508	-0.634	0.615
21	27	Club_21_27	0.539^{***}	0.450	0.622
21	28	Club_21_28	0.425	-0.746	0.622
21	29	Club_21_29	0.463^{***}	0.270	0.926
21	30	Club_21_30	0.483^{***}	0.357	0.627
21	31	Club_21_31	-0.891^{***}	-1.211	-0.768
21	32	Club_21_32	-0.794^{***}	-1.243	-0.707
21	33	Club_21_33	-0.831^{***}	-1.168	-0.703
21	34	Club_21_34	-0.876^{***}	-1.155	-0.780
21	35	Club_21_35	-0.901^{***}	-1.272	-0.773
21	36	Club_21_36	-1.360^{***}	-1.825	-1.193
21	37	Club_21_37	-1.212^{***}	-1.746	-0.915
21	38	Club_21_38	-1.190^{***}	-1.908	-0.912
21	39	Club_21_39	-0.895^{***}	-1.522	-0.761
21	40	Club_21_40	-0.862^{***}	-1.101	-0.731
22	23	Club_22_23	-0.601^{***}	-0.674	-0.547
22	24	Club_22_24	-0.228	-0.683	0.102
22	25	Club_22_25	0.480^{***}	0.410	0.587
22	26	Club_22_26	0.513	-0.701	0.539
22	27	Club_22_27	0.542^{*}	-0.692	0.591
22	28	Club_22_28	0.434	-0.739	0.552
22	29	Club_22_29	0.479	-0.656	0.920
22	30	Club_22_30	0.489^{***}	0.225	0.546
22	31	Club_22_31	-0.835^{***}	-0.938	-0.631
22	32	Club_22_32	-0.729^{***}	-0.787	-0.583
22	33	Club_22_33	-0.779^{***}	-0.849	-0.599
22	34	Club_22_34	-0.816^{***}	-0.913	-0.599
22	35	Club_22_35	-0.853^{***}	-1.021	0.116

Continued on next page

Club1	Club2	Label	$\hat{\theta}_{gh}$	bca_lo	bca_hi
22	36	Club_22_36	-1.307^{***}	-1.502	-0.675
22	37	Club_22_37	-1.144^{***}	-1.360	-0.583
22	38	Club_22_38	-1.132^{***}	-1.435	-0.608
22	39	Club_22_39	-0.843^{**}	-1.022	0.378
22	40	Club_22_40	-0.794^{***}	-0.900	0.130
23	24	Club_23_24	-0.003	-0.101	0.316
23	25	Club_23_25	0.555^{***}	0.551	0.613
23	26	Club_23_26	0.578^{***}	0.488	0.615
23	27	Club_23_27	0.585^{***}	0.533	0.622
23	28	Club_23_28	0.540^{*}	-0.538	0.589
23	29	Club_23_29	0.703^{***}	0.644	0.921
23	30	Club_23_30	0.566^{***}	0.512	0.632
23	31	Club_23_31	-0.887^{***}	-1.195	-0.734
23	32	Club_23_32	-0.744^{***}	-0.998	-0.656
23	33	Club_23_33	-0.807^{***}	-0.950	-0.488
23	34	Club_23_34	-0.865^{***}	-1.149	-0.782
23	35	Club_23_35	-0.901^{***}	-1.282	-0.773
23	36	Club_23_36	-1.479^{***}	-1.837	-1.327
23	37	Club_23_37	-1.333^{***}	-1.739	-0.991
23	38	Club_23_38	-1.282^{***}	-1.625	-0.812
23	39	Club_23_39	-0.893^{***}	-1.287	-0.768
23	40	Club_23_40	-0.842^{***}	-1.063	-0.716
24	25	Club_24_25	0.588^{***}	-0.239	0.625
24	26	Club_24_26	0.605^{***}	0.306	0.624
24	27	Club_24_27	0.602^{***}	0.306	0.620
24	28	Club_24_28	0.589^{***}	0.306	0.608
24	29	Club_24_29	0.783^{**}	-0.463	0.926
24	30	Club_24_30	0.599^{***}	-0.126	0.626
24	31	Club_24_31	-0.469^{*}	-1.038	-0.049

Continued on next page

Club1	Club2	Label	$\hat{\theta}_{gh}$	bca_lo	bca_hi
24	32	Club_24_32	-0.262	-0.875	0.085
24	33	Club_24_33	-0.425^{*}	-0.989	-0.036
24	34	Club_24_34	-0.419	-1.122	0.315
24	35	Club_24_35	-0.553	-1.260	0.550
24	36	Club_24_36	-1.080^{**}	-1.814	0.306
24	37	Club_24_37	-0.797^{*}	-1.724	-0.091
24	38	Club_24_38	-0.837	-1.597	1.092
24	39	Club_24_39	-0.510	-1.033	1.218
24	40	Club_24_40	-0.331	-1.043	0.646
25	26	Club_25_26	0.620^{***}	0.545	0.630
25	27	Club_25_27	0.614^{**}	-0.556	0.623
25	28	Club_25_28	0.617^{*}	-0.611	0.625
25	29	Club_25_29	0.682^{***}	0.017	0.926
25	30	Club_25_30	0.618^{***}	0.310	0.626
25	31	Club_25_31	0.434^{***}	0.394	0.535
25	32	Club_25_32	0.499^{***}	0.448	0.564
25	33	Club_25_33	0.434^{***}	0.384	0.552
25	34	Club_25_34	0.456^{***}	0.313	0.620
25	35	Club_25_35	0.383	-0.737	0.651
25	36	Club_25_36	0.248^{*}	-0.016	0.523
25	37	Club_25_37	0.392^{***}	0.340	0.611
25	38	Club_25_38	0.347^{*}	0.271	1.092
25	39	Club_25_39	0.411	0.146	1.216
25	40	Club_25_40	0.490^{***}	0.377	1.068
26	27	Club_26_27	0.620^{***}	0.615	0.628
26	28	Club_26_28	0.626^{***}	0.626	0.630
26	29	Club_26_29	0.685^{***}	0.691	0.920
26	30	Club_26_30	0.626^{***}	0.625	0.629
26	31	Club_26_31	0.474	-1.181	0.507

Continued on next page

Club1	Club2	Label	$\hat{\theta}_{gh}$	bca_lo	bca_hi
26	32	Club_26_32	0.530	-0.895	0.569
26	33	Club_26_33	0.473	-1.257	0.518
26	34	Club_26_34	0.492	-1.061	0.514
26	35	Club_26_35	0.428	-1.019	0.451
26	36	Club_26_36	0.312	-1.815	0.359
26	37	Club_26_37	0.438	-1.741	0.523
26	38	Club_26_38	0.398	-1.892	0.463
26	39	Club_26_39	0.453	-1.531	0.499
26	40	Club_26_40	0.522	-1.052	0.573
27	28	Club_27_28	0.618^{***}	0.616	0.620
27	29	Club_27_29	0.657^{***}	0.487	0.926
27	30	Club_27_30	0.619^{***}	0.506	0.620
27	31	Club_27_31	0.517^{***}	0.386	0.621
27	32	Club_27_32	0.553^{***}	0.452	0.622
27	33	Club_27_33	0.516	-0.949	0.620
27	34	Club_27_34	0.529	-1.143	0.586
27	35	Club_27_35	0.486	-1.270	0.568
27	36	Club_27_36	0.408	-1.814	0.620
27	37	Club_27_37	0.494^{***}	0.324	0.622
27	38	Club_27_38	0.467^{***}	0.234	0.622
27	39	Club_27_39	0.503	-1.029	0.638
27	40	Club_27_40	0.549	-1.032	0.632
28	29	Club_28_29	0.717^{***}	0.623	0.926
28	30	Club_28_30	0.625^{***}	0.623	0.632
28	31	Club_28_31	0.368	-1.217	0.520
28	32	Club_28_32	0.459	-1.225	0.566
28	33	Club_28_33	0.368	-1.234	0.530
28	34	Club_28_34	0.397	-1.164	0.549
28	35	Club_28_35	0.299	-1.285	0.530

Continued on next page

Club1	Club2	Label	$\hat{\theta}_{gh}$	bca_lo	bca_hi
28	36	Club_28_36	0.111	-1.838	0.429
28	37	Club_28_37	0.304	-1.743	0.528
28	38	Club_28_38	0.244	-1.914	0.476
28	39	Club_28_39	0.336	-1.629	0.550
28	40	Club_28_40	0.446	-1.080	0.623
29	30	Club_29_30	0.694^{***}	0.558	0.811
29	31	Club_29_31	0.355^{*}	0.162	0.926
29	32	Club_29_32	0.531^{***}	0.261	0.923
29	33	Club_29_33	0.356	-0.044	0.922
29	34	Club_29_34	0.410	-0.837	0.922
29	35	Club_29_35	0.233	-0.864	0.832
29	36	Club_29_36	-0.094	-1.194	0.923
29	37	Club_29_37	0.234	-0.183	0.922
29	38	Club_29_38	0.130	-0.148	0.977
29	39	Club_29_39	0.297	-0.824	0.996
29	40	Club_29_40	0.507^{**}	-0.025	0.953
30	31	Club_30_31	0.442^{***}	0.316	0.625
30	32	Club_30_32	0.508^{***}	0.415	0.627
30	33	Club_30_33	0.442^{***}	0.298	0.625
30	34	Club_30_34	0.464	-0.801	0.525
30	35	Club_30_35	0.390	-0.863	0.478
30	36	Club_30_36	0.252	-0.310	0.403
30	37	Club_30_37	0.399^{***}	0.217	0.626
30	38	Club_30_38	0.353^{***}	0.189	0.630
30	39	Club_30_39	0.418^{***}	0.157	0.627
30	40	Club_30_40	0.500^{***}	0.289	0.628
31	32	Club_31_32	-0.971^{***}	-1.168	-0.827
31	33	Club_31_33	-0.972^{***}	-1.071	-0.802
31	34	Club_31_34	-1.032^{***}	-1.114	-0.802

Continued on next page

Club1	Club2	Label	$\hat{\theta}_{gh}$	bca_lo	bca_hi
31	35	Club_31_35	-1.025^{***}	-1.168	0.099
31	36	Club_31_36	-1.465^{***}	-1.747	-1.125
31	37	Club_31_37	-1.359^{***}	-1.509	-1.021
31	38	Club_31_38	-1.318^{***}	-1.579	-0.995
31	39	Club_31_39	-1.031^{***}	-1.272	-0.407
31	40	Club_31_40	-1.039^{***}	-1.175	-0.834
32	33	Club_32_33	-0.899^{***}	-1.013	-0.817
32	34	Club_32_34	-0.960^{***}	-1.174	-0.884
32	35	Club_32_35	-0.969^{***}	-1.253	-0.766
32	36	Club_32_36	-1.477^{***}	-1.823	-1.117
32	37	Club_32_37	-1.353^{***}	-1.708	-0.945
32	38	Club_32_38	-1.306^{***}	-1.637	-0.902
32	39	Club_32_39	-0.970^{***}	-1.304	-0.824
32	40	Club_32_40	-0.957^{***}	-1.158	-0.836
33	34	Club_33_34	-0.963^{***}	-1.067	-0.861
33	35	Club_33_35	-0.970^{***}	-1.074	0.204
33	36	Club_33_36	-1.397^{***}	-1.574	-0.903
33	37	Club_33_37	-1.274^{***}	-1.438	-0.892
33	38	Club_33_38	-1.245^{***}	-1.544	-0.914
33	39	Club_33_39	-0.971^{*}	-1.075	1.219
33	40	Club_33_40	-0.961^{***}	-1.061	-0.148
34	35	Club_34_35	-1.020^{***}	-1.125	0.281
34	36	Club_34_36	-1.483^{***}	-1.615	-0.974
34	37	Club_34_37	-1.376^{***}	-1.525	-0.997
34	38	Club_34_38	-1.330^{***}	-1.633	-0.980
34	39	Club_34_39	-1.026^{***}	-1.063	0.416
34	40	Club_34_40	-1.033^{***}	-1.066	0.183
35	36	Club_35_36	-1.402^{***}	-1.599	-0.576
35	37	Club_35_37	-1.295^{***}	-1.482	-0.148

Continued on next page

Club1	Club2	Label	$\hat{\theta}_{gh}$	bca_lo	bca_hi
35	38	Club_35_38	-1.267^{***}	-1.584	-0.184
35	39	Club_35_39	-1.021^{**}	-1.202	0.645
35	40	Club_35_40	-1.025^{***}	-1.184	0.187
36	37	Club_36_37	-1.742^{***}	-1.790	-1.352
36	38	Club_36_38	-1.667^{***}	-1.864	-1.205
36	39	Club_36_39	-1.434^{***}	-1.821	-1.106
36	40	Club_36_40	-1.534^{***}	-1.826	-1.133
37	38	Club_37_38	-1.634^{***}	-1.839	-1.201
37	39	Club_37_39	-1.326^{***}	-1.722	-0.473
37	40	Club_37_40	-1.433^{***}	-1.736	-1.049
38	39	Club_38_39	-1.292^{***}	-1.704	-0.390
38	40	Club_38_40	-1.372^{***}	-1.884	-0.992
39	40	Club_39_40	-1.031^{***}	-1.313	-0.376

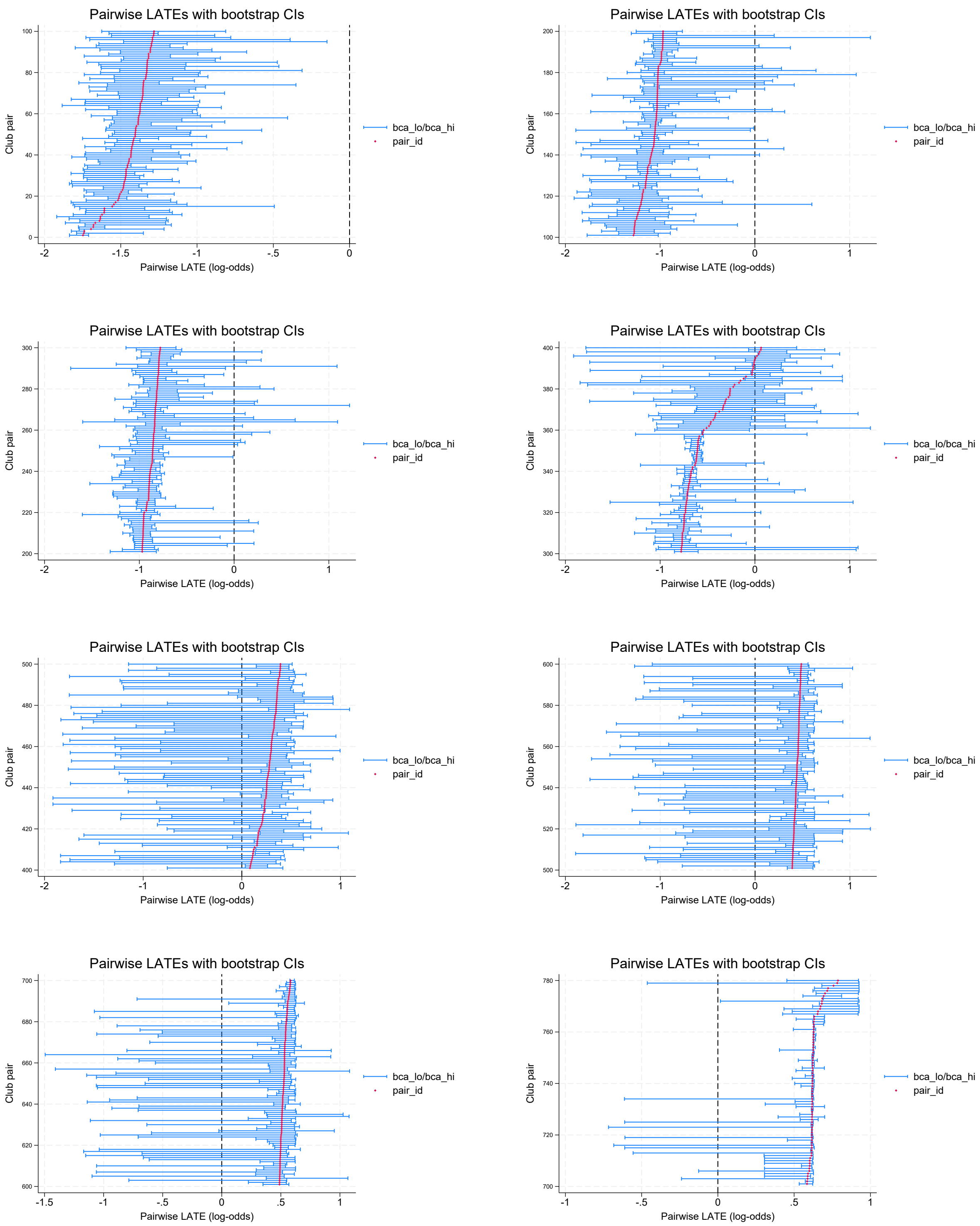

Figure B.1: Pairwise LATE plots with BCa Bootstrap CI for the subgroup of 5, 720 SNPs.

Table B.3: The effect of education on smoking: MR-Egger, IVW, and Plurality rule

	(1) Wald ratio	(2) MR Egger	(3) IVW	(4) Plurality
Years of education (std)	0.000	2.244***	-0.083***	0.236***
	(0.011)	(0.032)	(0.011)	(0.023)
N	5720	5720	5720	1012

Notes: Standard errors in parentheses. * $p < 0.1$, ** $p < 0.05$, *** $p < 0.01$.